# REPUBLIC OF TURKEY YILDIZ TECHNICAL UNIVERSITY GRADUATE SCHOOL OF NATURAL AND APPLIED SCIENCES

# HUMAN FALL DETECTION USING NON-CONTACT RADAR SENSOR

### Khadija HANIFI

MASTER OF SCIENCE THESIS

Department of Computer Engineering

Program of Computer Engineering

Advisor Assoc. Prof. Dr. M.Elif KARSLIGİL

# REPUBLIC OF TURKEY YILDIZ TECHNICAL UNIVERSITY GRADUATE SCHOOL OF NATURAL AND APPLIED SCIENCES

### HUMAN FALL DETECTION USING NON-CONTACT RADAR SENSOR

A thesis submitted by Khadija HANIFI in partial fulfillment of the requirements for the degree of **MASTER OF SCIENCE** is approved by the committee on 14.02.2020 in Department of Computer Engineering, Program of Computer Engineering .

Assoc. Prof. Dr. M.Elif KARSLIGİL Yildiz Technical University Advisor

Approved By the Examining Committee	
Assoc. Prof. Dr. M.Elif KARSLIGİL, Advisor Yildiz Technical University	
Prof. Dr. Yusuf SİNAN AKGÜL, Member Gebze Technical University	
Assoc. Prof. Dr. Gökhan BİLGİN, Member Yildiz Technical University	

I hereby declare that I have obtained the required legal permissions during data collection and exploitation procedures, that I have made the in-text citations and cited the references properly, that I have not falsified and/or fabricated research data and results of the study and that I have abided by the principles of the scientific research and ethics during my Thesis Study under the title of Human Fall Detection Using Non-Contact Radar Sensor supervised by my supervisor, Assoc. Prof. Dr. M.Elif KARSLIGİL. In the case of a discovery of false statement, I am to acknowledge any legal consequence.

Khadija HANIFI

Signature

Dedicated to children of Syria Seeds of peace...

### **ACKNOWLEDGEMENTS**

I would first like to express my sincere gratitude to my thesis advisor Assoc. Prof. Dr. Elif KARSLIGIL for the continuous support of this thesis, for her patience, motivation, and immense knowledge. Her guidance helped me all the time during research and writing this thesis. I do not imagine having a better advisor and mentor for my thesis study.

Besides my advisor, I would like to thank my colleague Dr. Ramin Fadaei FOULADI for his insightful comments and encouragement, and also for the hard questions which incented me to widen my research from various perspectives.

A very special gratitude goes out to my team leaders at ARÇELIK Sensor Technologies RD: Dr. Murat KANTAŞ and Dr. Bekir ÖZYURT who provided me the opportunity to join their team, and who gave access to their laboratory and research facilities. Without their precious support it would not be possible to conduct this work.

With a special mention to my colleagues and friends in Arçelik: Dr. Ismet ARSAN, Ali NAGARİA and Tayyab WAQAR for sharing their valuable experiences with me, and for their unfailing support and assistance.

I am grateful to my mother Yana, who have provided me through moral and emotional support in whole my life. She was always keen to know what I was doing and how I was proceeding, although it is likely that she has never grasped what it was all about! I am also grateful to my other family members and friends who have supported me along the way.

Last but by no means least, I must express my very profound gratitude to my significant other, Ali Hüseyin RÜSTEM who was always there for me whenever he thought I needed him. He always liked doing favors for me because it is his way of showing me how much he cared about me and how important I am to him. I owe it all to you. Many Thanks!

Khadija HANIFI

## TABLE OF CONTENTS

LI	ST O	SYMBOLS	vii
LI	ST O	ABBREVIATIONS	viii
LI	ST O	FIGURES	xi
LI	ST O	TABLES	xiii
ΑF	3STR	СТ	xiv
ÖZ	ZET		xv
1	INT	ODUCTION	1
	1.1	Literature Review	2
		1.1.1 Characteristics of Fall	2
		1.1.2 Approaches of Fall Detection	4
		1.1.3 Fall Detection Using Radar	8
	1.2	Objective of the Thesis	14
	1.3	Hypothesis	14
2	SYS	EM ARCHITECTURE and DATA COLLECTION	15
	2.1	Doppler Radar Functioning Principle	15
	2.2	Hardware Architecture Overview	16
	2.3	Experimental Setup	18
	2.4	Data Collection	19
3	MET	HODOLOGY	23
	3.1	Pre-processing	24
	3.2	Sensing Major Physical Activities	24
	3.3	Fall Detection	25
		3.3.1 Features Extraction	25
		3.3.2 Data Visualization	31
		3.3.3 Feature Scaling	32
		3.3.4 Feature Evaluation and Selection	33

		3.3.5	Designing Classification Model	35
	3.4	Vital S	Signs Extraction	38
		3.4.1	Eliminating Noise and Artifacts	38
		3.4.2	Heart and Respiration Rates Extraction	40
		3.4.3	Reference Sensors	41
4	RES	ULTS a	nd DISCUSSION	43
	4.1	Vital S	Signs Monitoring	43
	4.2	Activit	ry Classification and Fall Detection	44
	4.3	Conclu	usion and Recommendations	53
A	EXT	RACTE	D FEATURES	56
RE	EFERI	ENCES		58
DΙ	IBLIC	ATION:	S from the THESIS	66

### LIST OF SYMBOLS

*f c* Cut-off Frequency

 $\Delta \theta$  Demodulated Waveform

x' Derivative of x

 $ar{k}$  DFT Sample Index

E(x) Expected Value

I In-phase

 $ar{f}$  Mean Frequency

 $\mu$  Mean Value

ŷ Predicted Label

Q Quadrature

Fs Sample Rate

x'' Second Derivative of x

 $\sigma$  Standard Deviation

 $\lambda$  Wavelength

### LIST OF ABBREVIATIONS

ADC Analog to Digital Converter

ANN Artificial Neural Networks

AUC Area Under the Curve

CV Cross Validation

CW Continuous Wave

DC Direct Current

DCT Discrete Cosine Transform

DFT Discrete Fourier Transform

DL Deep Learning

DNN Deep Neural Network

DT Decision tree

DWT Discrete Wavelet Transform

FFT Fast Fourier Transform

FIR Finite Impulse Response

FMCW Frequency-Modulated Continuous-Wave

FPR False Positive Rate

HR Heart Rate

HRRP High Resolution Range Profile

IR Infra-Red

ISAR Inverse Synthetic Aperture Radar

ISR Interrupt Service Routine

kNN k-Nearest Neighbor

LSTM Long-Short-Term Memory

LSVM Linear kernel SVM

MAE Mean Absolute Error

MC Modified CLEAN

MD Mahalanobis Distance

ME Max Envelope

MFCCs Mel-frequency Cepstral Coefficients

MPA Major Physical Activities

MPCA Multi-dimensional Principal Component Analysis

MPD Matching Pursuit Decomposition

NJR New Japan Radio

NMF Nonegative Matrix Factorization

PBC Power Burst Curve

RCR Range Control Radar

RCS Radar Cross-Section

RDT Randomized Decision tree

RF Radio Frequency

RFID Radio Frequency Identification

RMS Root Mean Squared

RNN Recurrent Neural Network

ROC Receiver Operator Characteristic

RR Respiration Rate

SFCW Stepped-Frequency Continuous Wave

SVM Support Vector Machine

t-SNE t-Distributed Stochastic Neighbor Embedding

TC Turns Count

TF Time-Frequency

TPR True Positive Rate

URFR UR Fall Detection Dataset

UWB Ultra-Wide-Band

WT Wavelet Transform

ZCR Zero Crossing Rate

## LIST OF FIGURES

Figure	1.1	Fatal fall rates by sex and age group per 100,000 population [5] .	1
Figure	1.2	Fall detection general workflow	4
Figure	1.3	Tri-axial accelerometer raw data[g] and extracted features J1, J2	
		and J3[17]	5
Figure	1.4	Imaging the pressure on floor: (a) different postures, (b) simulated	
		pressure images, and (c) related histogram of each pressure. [20]	6
Figure	1.5	State classification during the fall process[26]	6
Figure	1.6	Sensor used for fall detection before and after 2014[46]	8
Figure	1.7	Spectrogram based features example [82]	11
Figure	1.8	Usage percentages of different radar types	14
Figure	2.1	Doppler radar structure	16
Figure	2.2	Doppler radar structure with I/Q demodulation	16
Figure	2.3	Hardware architecture design	17
Figure	2.4	Bandpass filter response	17
Figure	2.5	The setup of the experimental environment with two different	
		radar locations	18
Figure	2.6	Radar's field of view	19
Figure	2.7	Different scenarios followed while collecting data	21
Figure	2.8	Time and frequency domains corresponded to scenario $1 \dots \dots$	22
Figure	3.1	Fall detection system flowchart	23
Figure	3.2	RMS scores for different scenarios	25
Figure	3.3	Correlation Matrix Between Features	29
Figure	3.4	Significant Correlation Between Features	29
Figure	3.5	Correlation scores between time domain features	30
Figure	3.6	Correlation scores between time domain features (group 1)	31
Figure	3.7	Correlation scores between time domain features (group 2)	31
Figure	3.8	Correlation scores between time domain features (group 3)	32
Figure	3.9	Main steps followed for feature engineering	35
Figure	3.10	5 fold cross validation data sets separation	37
Figure	3.11	Noise and artefacts eliminating algorithm	39
Figure	3.12	Demodulated signal before and after artifact cancellation	39

Figure	3.13	Frequency domain response of the used FIR bandpass filters	40
Figure	3.14	Extracted and reference signals	41
Figure	3.15	HR and RR reference sensors and signals	42
Figure	4.1	Visualization of feature distribution using different metrics	45
Figure	4.2	Classification Results with all Features and Different Scaling	
		Algorithms	46
Figure	4.3	Classification results for different feature groups	46
Figure	4.4	Classification results with 30 sorted features	49
Figure	4.5	ROC curves and AUC scores for different classifiers on testSet3	50
Figure	4.6	Confusion matrices for fall detecting using different classifiers	51

## LIST OF TABLES

Table 1.1	Most cited papers on fall detection published since 2014	7
Table 1.2	Summary of radar based fall detection studies	10
Table 1.3	Comparison between most commonly used Doppler radar types	13
Table 2.1	Participated subjects details	20
Table 4.1	MAE and Accuracy results for different test sets	44
Table 4.2	Evaluation scores for each feature	47
Table 4.3	Evaluating results with different metrics on testSet1	52
Table 4.4	Evaluating results with different metrics on testSet2	52
Table 4.5	Evaluating results with different metrics on testSet3	52
Table 4.6	The average of evaluating results on the three test sets	53
Table A.1	Details of the extracted features	56
Table A.2	Features extracted from spectral power	57

### **Human Fall Detection Using Non-Contact Radar Sensor**

Khadija HANIFI

Department of Computer Engineering
Master of Science Thesis

Advisor: Assoc. Prof. Dr. M.Elif KARSLIGİL

Falling is the main cause of disability and fatality of elderly. In this work, 24 GHz continuous wave Doppler radar is used to develop a low price fall detection system. Radar sensor is selected due to its capability of tracking human motions, passing through covers and walls, its low cost, low power, and small size. Designed system is further improved to detect and monitor the human's vital signs to analyze the status of the fallen person and reduce the consequences of the fall by providing a general idea about the persons' situation to the concerned authorities. First, considering all possible daily activities and fall cases, a dataset with 121 fall and 117 non-fall signatures are collected. Then, features from both time and frequency domains are extracted and examined to select the ones that contribute most to distinguish between fall and non-fall samples. Finally, different machine learning techniques including support vector machine, naive Bayes, k nearest neighbor, linear discriminant analysis and decision tree are evaluated to build the most accurate classification model. Proposed system performed activity classification and fall detection with 88% average accuracy, heart rate monitoring with 95% average accuracy, and respiration rate monitoring with 85% average accuracy.

**Keywords:** Fall detection, vital signs, Doppler radar, machine learning, elderly care

YILDIZ TECHNICAL UNIVERSITY
GRADUATE SCHOOL OF NATURAL AND APPLIED SCIENCES

### Radar Sensörü ile Temassız Düşme Algılama

Khadija HANIFI

Bilgisayar Mühendisliği Anabilim Dalı Yüksek Lisans Tezi

Danışman: Doç. Dr. M.Elif KARSLIGİL

Düşme, yaşlıların sakatlık ve ölümünün ana nedenidir. Bu çalışmada, 24 GHz sürekli dalga Doppler radar sensör kullanarak yaşlı düşmesi tespiti için düşük fiyatlı bir sistem geliştirildi. Radari seçilme sebebi; insan hareketleri takip edebilmesi,duvarlardan geçebilmesi, düşük maliyet, düşük güç, ve küçük boyutlu gibi özeliklere sahip olması. Ayrıca, tasarlanan sistem, düşüşten sonra kişilerin durumunu incelemek ve ilk yanıtlayanlara gerekli bakım hakkında genel bir fikir sağlamak için , kişinin yaşamsal belirtileri takip etmek ve hesaplamak için geliştirilmiştir. İlk olarak, toplam 121 düşme örneği ve 117 düşme olamayan normal günlük aktivite örneğinden oluşan bir veri seti hazırladık. Sonra hem zaman hem de frekans alanlarından farklı özellikler çıkarıldı ve düşme ile düşme olmayan örnekleri en iyi ayırt eden olan özellikler kümesi seçildi. Son olarak, seçilen özellikler, destek vektör makinesi, naif Bayes, en yakın k komşusu, lineer diskriminant analizi ve karar ağacı algoritmaları gibi farklı sınıflandırma algoritmaları dikkate alınarak bir sınıflandırma modeli geliştirildi. Önerilen sistem düşme tespiti için %88, kalp atış hızı tespiti için %95 ve solunum hızı tespiti için %85 'e başarı oranlarına ulaştı.

**Anahtar Kelimeler:** Düşme algılama, yaşamsal belirtileri, Doppler radar, makine öğrenmesi, yaşlı bakımı

YILDIZ TEKNİK ÜNİVERSİTESİ FEN BİLİMLERİ ENSTİTÜSÜ

# 1 INTRODUCTION

Falls of elderly seniors are one of the major public health problems due to their main cause of disability and in some cases even death [1, 2]. According to [3], each year, one of three elderlies fall, and since most of the elderlies take care of themselves in their own home, when a fall happens, they have difficulty to get up by themselves even if there are no direct injuries. Research in [4] shows that 50% of elders who stayed more than an hour lying on the floor after fall, died in six months after the accident. Figure 1.1 shows statistical results of fatal falls in USA grouped by 5-year age and sex. Consequently, detecting and reporting the fall directly after the fall could help to reduce the risks of the fall and save lives by providing proper care and preventing the injuries from worsening [4].

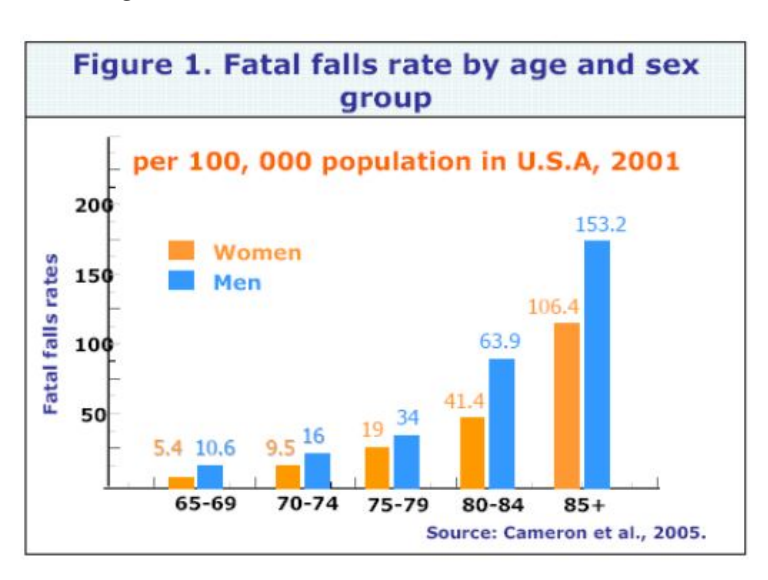


**Figure 1.1** Fatal fall rates by sex and age group per 100,000 population [5]

Driven by this demand, the detection of elderly falls have became an active area of research [6]. The most often used techniques in this field are associated with wearable devices, like accelerometers and "push buttons". The problems with these sensors are that they must be carried or worn, and they are intrusive and could be easily broken. Similarly, "push-button" based techniques are not practical for the cases when the user

is harmed [7].

More autonomous techniques based on non-wearable sensors such as passive cameras and infrared sensors have been developed. The shortcomings of these sensors are that they require very controlled placement, affected by lighting conditions, and obscured by walls and covers, besides, they raise safety and privacy matters [8].

To come over such problems, we considered utilizing radar sensor to design a system for elderly health monitoring and fall detection due to its capabilities of detecting human movements and passing through walls and fabrics, plus, its low cost, low power and small size [9]. Additionally, bathroom is considered where falls of elderly people are more likely to occur and yet other sensors, like cameras or acoustic sensors, are not suitable due to privacy concerns [10]. In this sense, radar represents the most suitable sensor.

Moreover, [11] presented a study about circumstances of elder falls at home. The results of analysing the falls of 414 individuals showed that half of the falls at home occurred in the bedroom and these falls were more common among individuals 70 years or older. After reviewing literature studies, it has been observed that most of the studies have paid less attention to bedroom fall cases. To cover this gasp, this study is conduct to focus more on bedroom related fall scenarios.

The rest of this chapter contains a comprehensive review on studies related to fall detection in the first section, then the objective of the thesis and the hypothesis are provided in second and third sections respectively.

### 1.1 Literature Review

To provide better organization and clearer assessment, the literature review discussion is divided into three main subsections: first, to better sense the problem, the characteristics and types of fall are identified. Then, approaches related to fall detection problem are discussed in detail in order to understand existed solutions and identify the unexplored area. Finally, approaches conducted to radar sensor are examined and evaluated.

#### 1.1.1 Characteristics of Fall

Before examining studies related to fall detection, all possible fall types and the characteristics of each type are first discussed. Identifying the fall characteristics is considered as a critical step not only because it is helpful to better understand existed

algorithms but also to discover existed gaps which leads us to come up with new solutions. Regarding this, in this section, the characteristics of different fall types are discussed with highlighting the most critical details.

Fall is an action which lasts between one and three seconds and the cause of fall could be related to different reasons such as health problems, lack of attention, and ageing. Since the characteristic of the fall varies according to the person and the ambient, specifying the characteristic of the fall is considered as a challenging task [12]. Thus, most of the studies that have been proposed to detect fall events have designed their systems according to their own tests and observations, and yet, researches that are considered to classify fall types are limited. However, examining the different fall types and the characteristic of each type is important to develop more proper solution. Study in [12] has aimed to classify fall types into three main categories: fall while sleeping (from bed), fall while sitting (from chair), and fall while walking or standing. The characteristics of each type are identified according to the sequences of its sub-actions as the following:

- 1. Characteristics of fall during sleep.
  - Initial status of the person: lying/sleeping on the bed.
  - Fall signature: the body falls in free manner from the bed height to the floor height.
  - Final position of the person: lying on the floor near the bed.
- 2. Characteristics of fall during sitting
  - Initial status of the person: sitting on a chair or couch.
  - Fall signature: the head falls in free manner and changes its height from the sitting height to the floor height.
  - Final position of the person: lying on the floor near the chair.
- 3. Characteristics of fall during walking/standing
  - Initial status of the person: lying or sleeping on the bed.
  - Fall signature: the body falls in free manner in one direction and the height of both the head and the body centers change from standing height to the floor height.
  - Final position of the person: lying on the floor within a circle which's centre is at the foot spot of the standing case and its radium is the height of the person.

Although fall could have different signatures, existing fall detection systems share a general work flow, as depicted in figure 1.2, and they differ in terms of complexity and limitations of utilized sensor.

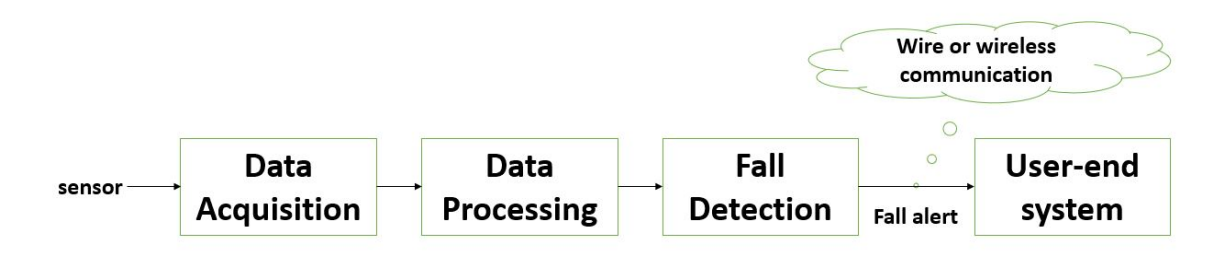


Figure 1.2 Fall detection general workflow

### 1.1.2 Approaches of Fall Detection

Over the last decade, fall detection problem has got a big attention from the community and plenty of effort has been made to provide more valuable fall detection products, likewise a lot of researches has been done to improve the efficiency of applied methods. The most critical criteria for building such a system are considered as: ease of usage, usability in different places, suitable for home usage, low price and high reliability. Literature researches done by [12] and [13] has divided fall detection approaches in accordance with the associated sensors into three main categories: wearable sensor-based approaches, ambient sensor-based approaches and vision sensor-based approaches. In this section an explanation about the used technologies and a brief compression between them is provided.

• Wearable sensor-based approaches: The most popular wearable sensor used in fall detection field is considered to be accelerometer. Accelerometer is used to measure and classify human physical movements, and it is not only the most used sensor, but also the initial sensor utilized for this aim. Early works on fall detection in [14] fallowed by [15] were based on data collected from accelerometer sensor which is replaced on the belt. The fall is identified in two steps: first the fall is detected by the impression of the shock on the floor, and then a mercury tilt is used to detect if the person is lying.

Lately, in [16] instead of using mercury tilt for detecting when the person is lying, a tri-axial accelerometer with three single-axis accelerometers oriented at 90 degrees to each other has been used. The sensor was placed in a mobile-phone to detect fall and other different daily activities. The advantage of using a tri-axial accelerometer over the usage of single-axis accelerometer; is to collect all three axes data at the same time. In [17], a tri-axial accelerometer has used to design

a real time device for elderly fall detection. The device is placed on the belt of the person to classify all kind of activities and detect falls. Figure 1.3 shows an example of the data gathered using accelerometer sensor in fall case, the raw data and the extracted three features for fall detection are presented. In [18], a 4-axis accelerometer unit has been designed to distinguish between falling events and normal activities such as fast walking and going up/downstairs.

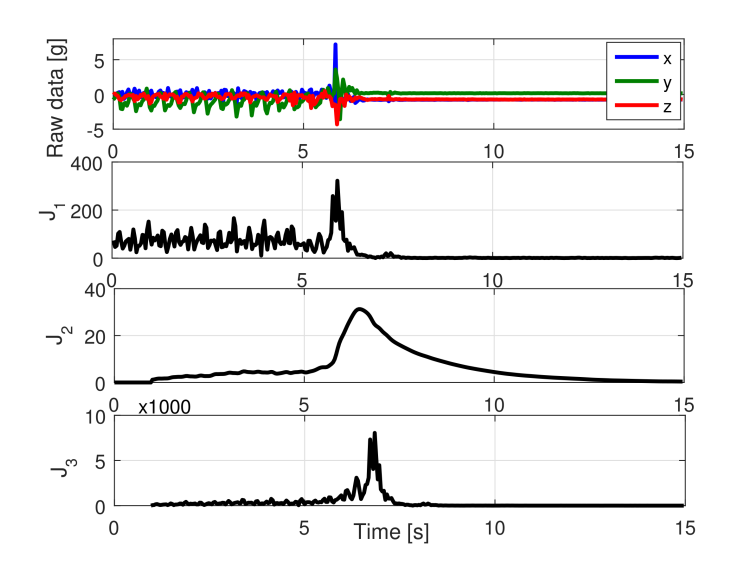


**Figure 1.3** Tri-axial accelerometer raw data[g] and extracted features J1, J2 and J3[17]

- Ambient sensor-based approaches: basically use multiple sensors to collect different kinds of data, such as vibration and audio data, and then fuse these data to detect falls. Detecting events and changes using vibrational data is useful in many ways like monitoring, tracking and localisation of the fall event, as in [19] where a floor vibration-based fall detection system has been designed. The system distinguishes between signatures generated by fall and others generated by daily normal activities, by monitoring the vibration signature of the floor. In [22], a product system for detecting falls from bed has been developed. The system involves two pressure sensors; one placed on the bed mattress to track bed entry and exist, and the other placed on the floor to monitor falls. In [20], a floor pressure imaging system using BackProjection algorithm embedded with fiber sensors has been designed. The aim of the developed system is to provide a suitable mat that could be used on the floor of a bathroom to detect all possible falls. Figure 1.4 presents examples of the classified activities.
- *Vision sensor-based approaches:* using vision sensors especially camera sensors has got a lot of researcher's attention in the last decade. Background extraction and tracking moving objects are the most common methods for vision-based fall detection. In [21] and [22], an Infra-Red (IR) sensor array replaced on the wall

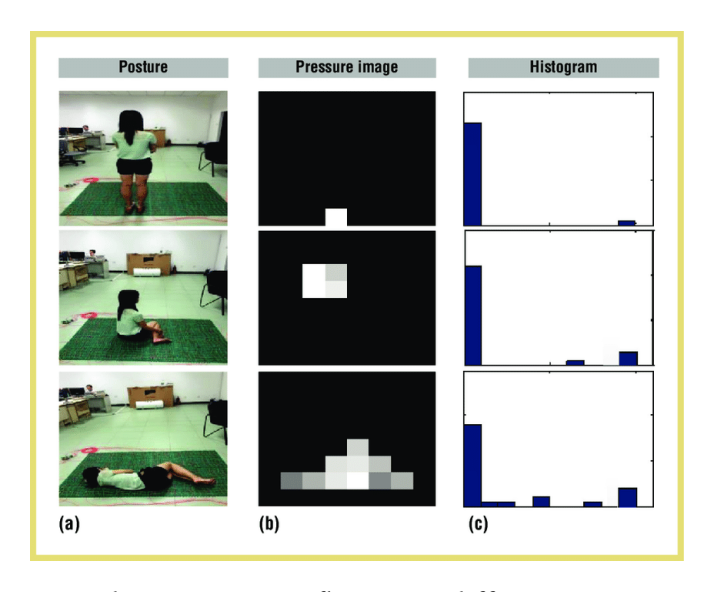


**Figure 1.4** Imaging the pressure on floor: (a) different postures, (b) simulated pressure images, and (c) related histogram of each pressure. [20]

is used to classify human activities and detect fall events. Then by analysing the size, location and the velocity of the moving object, activities and falls are detected. Other works have approached to detect falls with image processing techniques. For example, in [23], it has been proved that the vertical and the horizontal speeds during the fall are three times higher than any other activity. This inspired researches such as [24] and [25] to detect the fall by tracking the speed of the head movements. [26] proposed a single camera-based fall detection method for outdoor environment. Their method basically, captures images by an RGB camera generates a depth image using machine learning techniques, and then, the human form is detected and tracked for detecting fall events. Figure 1.5 represents the classification states they used for identifying the fall process.

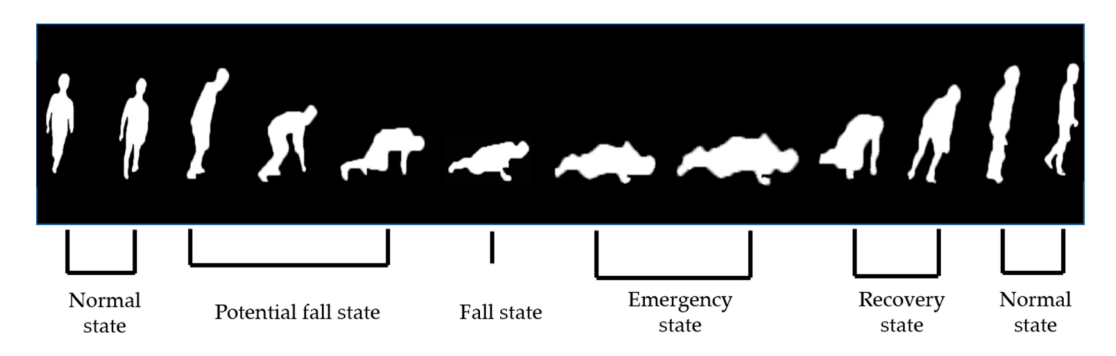


**Figure 1.5** State classification during the fall process [26]

All in all, to reflect the research trend of fall detection, the most popular research works over the last five years has been analysed. Papers in the fall detection field and that have been cited above 30 times has been selected and compared in table 1.1.

 Table 1.1 Most cited papers on fall detection published since 2014

Ref	Sensor	Method	Initial status	Participant (dataset)	Falls vs non-falls signatures	Acc
[27]	Kinect	DT	walking standing	13	454 vs 445	N/A
[28]	Kinect	Threshold SF	walking standing	3	12 vs 22	N/A
[29]	Tri-axial Accelerometer + Kinect	SVM	walking standing sitting	URFD	30 vs 402	98.3%
[30]	Accelerometer	Thresholds	walking standing	7	6 vs 7	97.5%
[31]	Kinect	Ad-hoc segmentation	walking standing	3	N/A	N/A
[32]	Kinect	SF ANN	walking standing	10 SDUFall*	30 vs 150	86.8%
[33]	Kinect	RDT SVM	walking standing	4	190 vs 190	97.6%
[34]	Radar	DWT	walking standing	1	19 vs 14	80%
[35]	Radar	DWT	walking standing	2	150 vs 704	89.8%
[36]	Accelerometer	SVM	walking standing	5	50 vs 50	92%
[37]	Kinect + Accelerometer	kNN SVM	walking standing	URFD	903 vs 1492	95.8%
[38]	Radar	DNN	walking standing	N/A	15 vs 45	87%
[39]	Kinect	kNN	walking standing sitting	URFD	66 vs 60	100%
[40]	tri-axial Accelerometer	Thresholds	walking standing sitting	11	231 vs 165	95 %
[41]	Accelerometer + camera	DT	walking standing	CAVIAR	N/A	79.5%
[42]	Kinect	NMF	walking standing sitting	2	50 vs 120	80%
[43]	Accelerometer	Thresholds	walking standing	10	13 vs 179	95.6%
[44]	Accelerometer	DT	walking standing	8	1879 vs 1611	97.5%
[45]	camera	SF	walking standing sitting	N/A	21 vs 30	90.5%

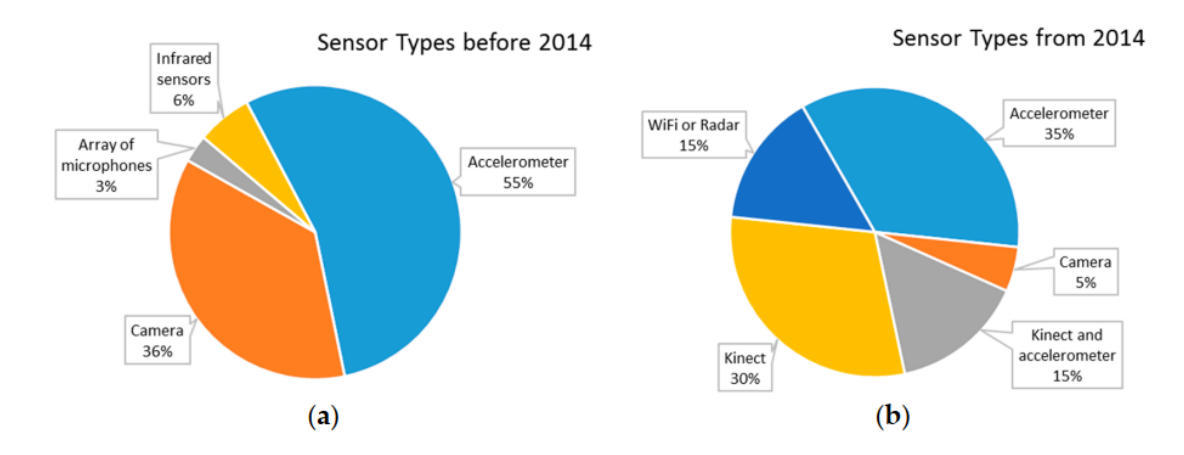


**Figure 1.6** Sensor used for fall detection before and after 2014[46]

Research presented in [46] and [47] have covered studies related to fall detection techniques and utilized sensor types. Their research results have showed 2014 as a division year in the sense of the sensors used for designing fall detection systems. Where new noncontact-based sensor types like radar and WiFi [48] started to get more attention and started being used in the fall detection field. These new sensors have the advantage of usage without the need for direct contact with the user and without violating the user's privacy. In figure 1.6, a summary about the sensors used for fall detection before and after 2014 is represented in the concept of pie charts. Study [46], categorized the sensors used for fall detection in three groups: first category is vision-based detectors which includes RGB cameras and depth cameras (Kinect is the most common depth sensor in this field), second category is accelerometer-based detectors which includes accelerometer devices and accelerometers built in smart phones, and the third category is radio frequency (RF) sensor-based detectors which covers radar and wi-fi based devices.

#### 1.1.3 Fall Detection Using Radar

Previously mentioned techniques including accelerometers, cameras and thermography, passive infrared sensors, and radio frequency identification (RFID) devices provide highly accurate results but they have several limitations such as; accelerometers require to be attached to human body, laser vibrometer requires very accurate control or placement, camera systems are affected by lighting conditions and obscured by walls and fabrics, besides, they raise privacy concerns. In this study in order to over come such problems, we considered radar as an alternative sensor to design non-wearable fall detector with no privacy concerns. Radar is an important technology used for elderly health monitoring and fall detection due to its capability of detecting human motions and passing through walls and ceilings in different rooms,

besides its low cost, low power and small size [49]. The main concept of radar-based systems is to transmit electromagnetic waves over a certain range of frequencies. When this wave strikes a moving object, it gets modulated by the object's movement and then it reflects in different directions. Radar's receiver detects this reflected signal and then by demodulating and analysing the reflected signal, movement components are extracted. Recently, various detection and classification techniques based on radar signals associated with body motions have been developed to identify falls from different motion states such as walking, standing, sitting, kneeling, etc. [50-56]. Mel-frequency cepstral coefficients (MFCCs) is considered as one of the most common feature extraction methods, it is commonly used for voice recognition methods to separate different voice sources. Some studies like [50], applied MFCC on radar signal to extract features related to body activities including fall. Another widely used method for feature extraction, used in [53–55], is the wavelet transform (WT), which extracts features from time-frequency signal. Extracted features are then classified by suitable machine learning method to distinguish between fall and non-fall motions. As it is shown in table 1.2, the most commonly used methods for fall and non-fall classification are SVM, DT and KNN.

Moreover, radar has proved highly accurate performance with vital signs detection which gives it the advantage over other sensor types to not only detect but also analyze the fall and define its type and cause. Also, by monitoring vital signs, radar is able to deliver a general idea about the person's situation after the fall which is very helpful for the first-responders to be prepared for the necessary care and treatments. However, using radar for fall detection has number of challenges such as:

- Daily activities like sitting and kneeling are more likely to be confused with falls and cause false alarms
- Pet jumping and fast movements could generate signatures like human falls.
- The presence of multiple persons in radar's field of view.

To increase the accuracy of fall detection system, studies like [57–59] have utilized multiple radar sensors to track subjects from more than one perspective. A data fusion is then performed either by feature selection or combination. Yet, using multiple sensors increases the system complexity and price. Instead, ultra-wideband (UWB) range-doppler radar sensor could be utilized to gather range information [60]. Range information is helpful to monitor more than one person in the field of view [61]. Using single sensor and multiple antenna is also a considered alternative to reduce noise and false alarms [50]. Radar based fall detection systems are basically developed by first

analysing the reflected RF signal and extracting a feature set, and then building a classification model based on the extracted feature set. Eventually, the accuracy of the classification results is highly affected by the type of the extracted features as it is also affected by the test environment and size of the training set. Table 1.2 represents a summary about studies made for fall detection using radar sensor. It is shown that, variety of feature sets with different test sizes and conditions have been proposed.

Table 1.2 Summary of radar based fall detection studies

Ref	Radar Type	Feature Extraction Method	Dataset	Classification Method(Acc %)
[57–59]	RCR	MFCC	109 falls 341 non-fall	SVM (93.0) kNN (96.0) NB (88.5)
[62–65]	CW+ dual-band planar	Spectrogram	20 walking 30 fall	LS-SVM (94.3)
[66]	CW + array sensor	MFCC	64 events	SVM (90.4)
[67–71]	CW+ wide-band sdr-kik	MPD PBC	20 fall 10 sitting standing 3)65 fall	SVM (100) SBL (85.0)
[72]	RCR	DWT	105 fall 704 non-fall	1- NN (83.0)
[73]	CW	ISAR image	N/A	frequency changing(N/A)
[74]	UWB	Phase info	N/A	HRRP (N/A)
[75, 76]	CW	1)PCA(Spect) 2)Spectrogram	15 fall 45 non-fall	SVM (73.0) DNN(87.0)
[77, 78]	UWB+ Kinect	Spectrogram	30 falls 406 non-falls	SVM (91.3) k-means (93.0)
[79]	UWB	DWT	NA	SVM (79.6%)
[80]	UWB	Sum of raw signal	121 falling 85 standing	LSVM (80.0) GSVM (79.1) KNN (78.6) DTW (83.5) LSTM (89.8)
[81]	UWB	MPCA	109 falling 105 sitting 95 bending 76 walking	kNN (96.6)

Approaches used to extract feature from Radar signals could be clustered as the bellow:

• *Spectrogram Based Features:* Spectrogram analysis is a commonly used technique for extracting time-frequency features. To analyze the frequency content of a finite duration discrete time signal x with N samples, Discrete Fourier Transform (DFT) is used:

$$\hat{x}(k) = \sum_{n=0}^{N-1} x(n)e^{-i\frac{2\pi k}{N}n}, k = 0, ...., N-1.$$
(1.1)

Taking DFT over a short period of time, will give a local snapshot in time of the frequency content of the signal. Thus, a sliding window is used for calculating the DFT; for instance, first taking the DFT of window x(1:m), then taking the DFT of x(2:m+1) window, and so on until end of the signal. This represents the spectrogram. The spectrogram is calculated using DFT as:

$$SPECTO(n,k) = \left| \sum_{m=1}^{N} x(n+m)h(m)e^{-i\frac{2\pi k}{N}m} \right|^{2},$$
 (1.2)

where h(m) is a window function –mostly Hanning window are used- to smooth the signal and increase time and frequency resolutions. Spectrogram is helpful to separate different motions by generating time-frequency signature for each motion. In [82], three time-frequency features -extreme frequency, torso frequency and event's length- are used for detecting human falls. Figure 1.7 shows these features in the spectrogram of a fall event.

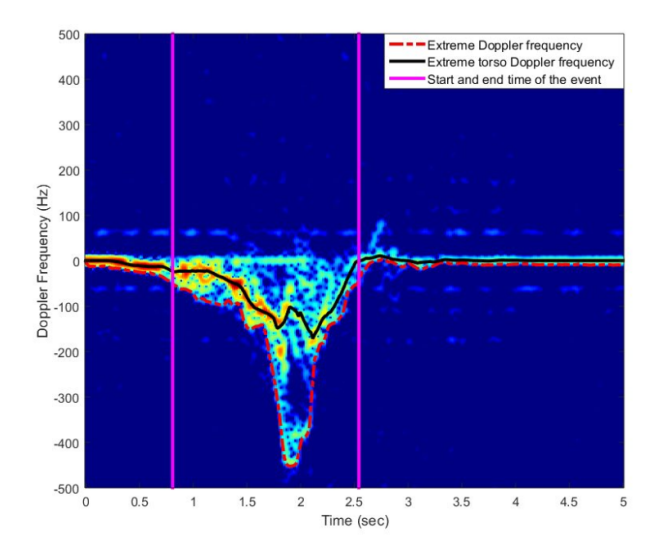


**Figure 1.7** Spectrogram based features example [82]

• *Mel-Frequency Cepstrum Coefficients (MFCC) Features:* MFCC is a commonly used method for voice feature extraction in speech recognition studies. Steps used for extracting MFCC features are: 1) the signal is divided into short frames. 2) the power spectrum of each frame is calculated. 3) mel filterbank is applied to the power spectra and the energy in each filter is summed. 4) logarithm of all

filterbank energies is taken. 5) discrete cosine transform (DCT) is applied. 6) first 2-13 DCT coefficients are kept and the rest are discarded. The mel-scale is a perceptual scale of pitches judged by listeners to make the features be more similar to human hearing. And since human ear interpretation of a pitch is linearly in the frequencies bellow 1000 Hz and logarithmically above 1000 Hz, the logarithmic scale is taken. As most of the energy in speech signals is in lower frequency bands, mel filter banks are designed to be narrow at low frequencies and board at high frequencies. Recently, MFCC has been utilized to extract fall and other body motions features. However, speech signals are different from fall signals in since of frequency rates and limits and parameters like mel scale limits used for speech signals cannot be utilized for fall signals but should be chosen to suit the analysed signal characteristics and cover observed frequency bands.

• *Discrete Wavelet Transform (DWT) Features*: WT is a technique of extracting both frequency and location features of a signal by applying a chain of pairs of low and high pass filters to it. The utilization of multiple filtering stages provides the flexibility to detect the exact frequency band by which the best resolution could be handled. The WT of a signal x(n) is computed as:

$$X(i,a) = \frac{1}{\sqrt{a}} \sum_{n} x(n) f^*(\frac{i-n}{a})$$
(1.3)

where f is wavelet function, a is scale factor, i denotes the translation, and  $\frac{1}{\sqrt{a}}$  is energy normalization factor.

• *Power Burst Curve (PBC) Features:* PBC represents the total power of the signal between a specific frequency band [f1, f2] at time instant kT, PBC values over slow time are used as a feature vector for classification, it is expressed as:

$$PBC(k) = \sum_{\nu; \nu F \ni [f_1, f_2]} |X[k, \nu]|^2 + \sum_{\nu; \nu F \ni [-f_1, -f_2]} |X[k, \nu]|^2$$
(1.4)

- *Inverse Synthetic Aperture Radar (ISAR) Features:* ISAR images are obtained by deriving the speed of the subject and plotting it with the radar cross-section range (RCS) information [73].
- *Matching Pursuit Decomposition (MPD) Features:* MPD is a time-frequency analysis technique used for signal decomposition [67]. In MPD, function segments or "atom" are matched to portions of the signal. The best matched atom is determined and extracted from the signal. Then the algorithm proceeds

to the next iteration. By this, the highest energy possible in each iteration is extracted.

Literature research shows that the most commonly used Doppler radar types for this problem are:

- *CW Doppler radar*: compares the frequency of received signal to the transmitted one and extracts only velocity information. In a CW Doppler radar system, the transmitter and the receiver are operating all the time. Therefore, to prevent transmitted and received signals from jamming each other, low transmit power levels are used, and this limits the distance in which it can detect a target. Because of its simple architecture, its cost is very low.
- *Pulse-Doppler range control radar (RCR):* combines Doppler processing to pulse radar to describe the rate that the subject is moving toward or away from the radar.
- *Ultra wide band radar (UWB):* is a pulsed radar system that generates a sequence of pulses of finite duration. In the times between pulses, the transmitter is not powered, whereas, the receiver is powered. So, it detects reflected signals by any objects. However, this advanced technology caused UWB radar to have the highest price in the marked compared to other Doppler radars.

Table 1.3 presents a compassion between these radars from the prospective of extracted information about the moving targets in their field of view

**Table 1.3** Comparison between most commonly used Doppler radar types

Feature	CW	RCR	UWB
Velocity	Yes	Yes	Yes
Direction	No	Yes	Yes
Multiple Targets	No	No	Yes
Cost	Low	Mid	High

By computing the usage percentages of each sensor in the literature, as shown in figure 1.8(a), it is observed that UWB radar is the most commonly used and studies that have used CW radar are very limited. The reason behind this bias is related to the more advanced technology that UWB sensor provides. However, the disadvantage of this sensor is its high price comparing to the CW radar. Furthermore, as it is shown in figure 1.8(b), 71% of the studies have used additional sensor, where 31% of them used more than one radar sensor and 40% used radar data and data extracted from other sensor type like kinect or array sensor.

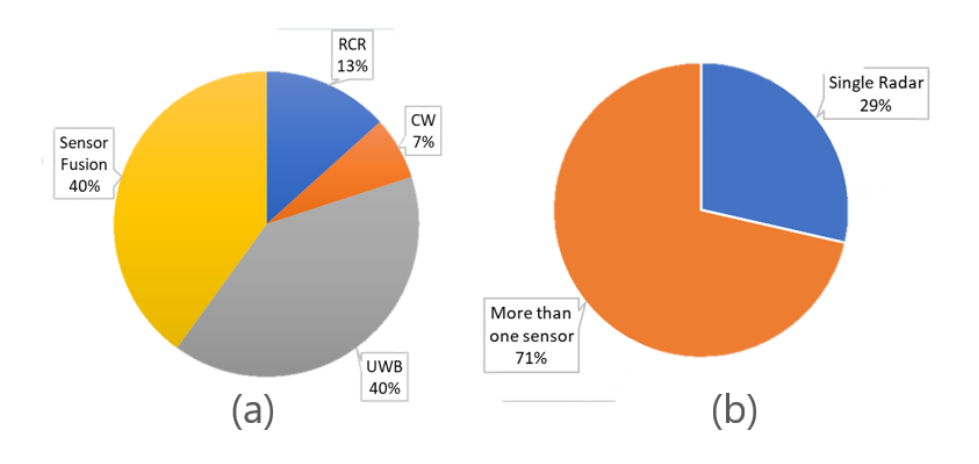


Figure 1.8 Usage percentages of different radar types

### 1.2 Objective of the Thesis

The objective of this study is to develop a contactless fall detection system based on Doppler radar sensor. The aim is to design system that is not only capable to detect the fall but also analyse the cause and the consequences of the fall, which is possible by monitoring the vital signs after the a fall is detected. The motivation of keep tracking the person after fall, is to update the concerned authorities about the senior's status to prevent more damage could be led or prevent panics caused by falls alarms.

### 1.3 Hypothesis

We believe that the ideal fall detection system to reduce the consequences of elderly falls is: contactless, passes through covers, not affected by light conditions, does not cause privacy violation problems, able to examine the condition of the fallen person by monitoring his/her vital signs after the fall, and affordable to low and middle income segments where fall is more likely to happen.

### SYSTEM ARCHITECTURE and DATA COLLECTION

This chapter focuses on explaining the designed fall detection system explaining the work principle of Doppler radar sensor, the hardware architecture, experimental setup, and the data collection protocols performed in this thesis.

### 2.1 Doppler Radar Functioning Principle

Radar systems are used to extract speed, distance and direction of objects using electromagnetic waves [83]. In microwave Doppler monitoring, the radar transmits a single tone with frequency f, the signal is then reflected from objects in the coverage area. Radar receives a signal like the transmitted one, with its phase modulated by the object's movement and by demodulating the signal, movement information are extracted. Considering  $\phi(t)$  the phase noise inside the microwave oscillator. Transmitted signal s(t) and received signal r(t) are represented in equations 2.1 and 2.2 respectively.

$$s(t) = \cos(wt + \phi(t)) \tag{2.1}$$

$$r(t) = cos(wt + \phi'(t) + \Delta\theta)$$
 (2.2)

Where  $\Delta\theta = 4pi * x(t)/\lambda$  is the phase shift caused by the motion. Here x(t) is the time varying displacement and  $\lambda$  is the wavelength of the transmitted signal. When the change in the displacement x(t), is small compared to  $\lambda$ , the phase change will be small. In this situation, phase modulated signal can be directly demodulated by mixing it with a portion of the original signal [84], as in equation 2.3:

$$sin(wt + \phi'(t) + \Delta\theta) * cos(wt + \phi(t)) = sin(\Delta\theta) + HFT$$
 (2.3)

where HFT is high frequency terms and  $sin(\Delta\theta) \approx \Delta\theta$  for small  $\Delta\theta$  [84].

Demodulated waveform  $\Delta\theta$  carries information about the motions of the object which the signal is reflected from. This structure is presented figure 2.1.

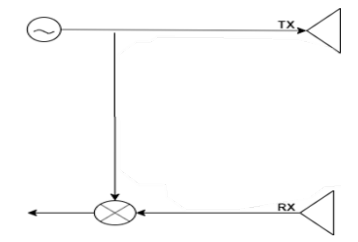
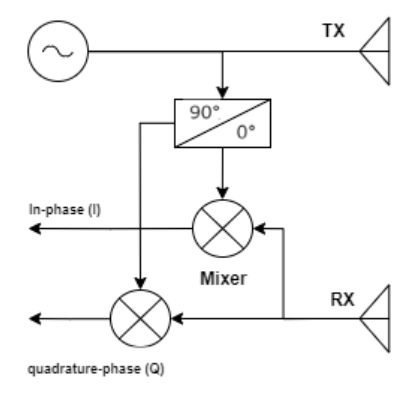


Figure 2.1 Doppler radar structure

However, when the distance between radar and the object is multiple of  $\pi$ , the baseband signal becomes null and extracting movement information is no longer possible. This is problem is referred as the null point problem [85]. To overcome the null detection problem, I/Q demodulation topology is used [86]. It provides two outputs; in-phase and quadrature signals with 90-degree phase difference. By this, when one signal is null, motion could be extracted form the other. Updated radar architecture is presented in figure 2.2.



**Figure 2.2** Doppler radar structure with I/Q demodulation

Generated I and Q signals are represented in equations 2.4 and 2.5 respectively. Then, the baseband signal is computed by using arc-tangent demodulation method.

$$I(t) = \cos(4\pi x(t)/\lambda + \phi_n(t) + \phi)$$
 (2.4)

$$Q(t) = \sin(4\pi x(t)/\lambda + \phi_n(t) + \phi)$$
 (2.5)

### 2.2 Hardware Architecture Overview

A practical, low-cost and easy implemented prototype system is designed, a block diagram of the prototype components is presented in figure 2.3, the system uses a low-cost K-band 24-GHz continuous wave Doppler radar transceiver sensor as the

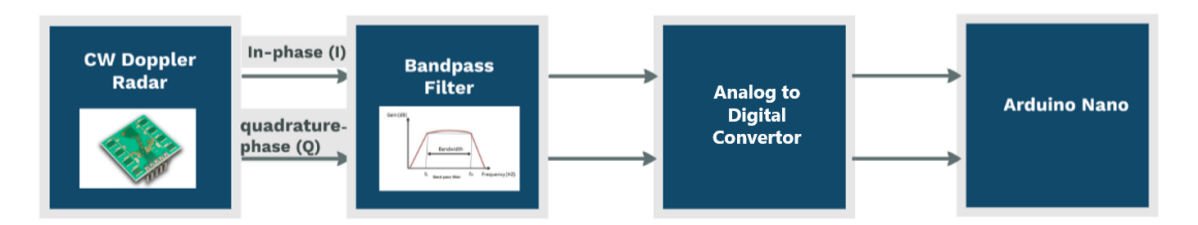


Figure 2.3 Hardware architecture design

main sensor. The radar provides two output signals I and Q, which are passed through an analog bandpass filter to pass frequencies related to heartbeat, respiration harmonics and random body movements with attenuating undesired components. For this end, a second order active band pass filter using inverting operational amplifier is designed, filter circuit is shown in figure 2.4, filter's lower cut-off frequency (fc1=0.5 Hz) and upper cut-off frequency (fc2 = 150 Hz) are presented in equations 2.6 and 2.7 respectively. The gain of the passed frequencies, as presented in equation 2.8, is 23db which is about 14 amplification level.

$$f_L = \frac{1}{(2\pi * R1 * C1)} = 0.5Hz \tag{2.6}$$

$$f_H = \frac{1}{(2\pi * R4 * C4)} = 150Hz \tag{2.7}$$

$$Gain = -\frac{R4}{R1} \tag{2.8}$$

Filtered signals are then converted from analog to digital. The signal is then sampled each 4 milliseconds (Fs = 250 Hz) and stored to be further processed.

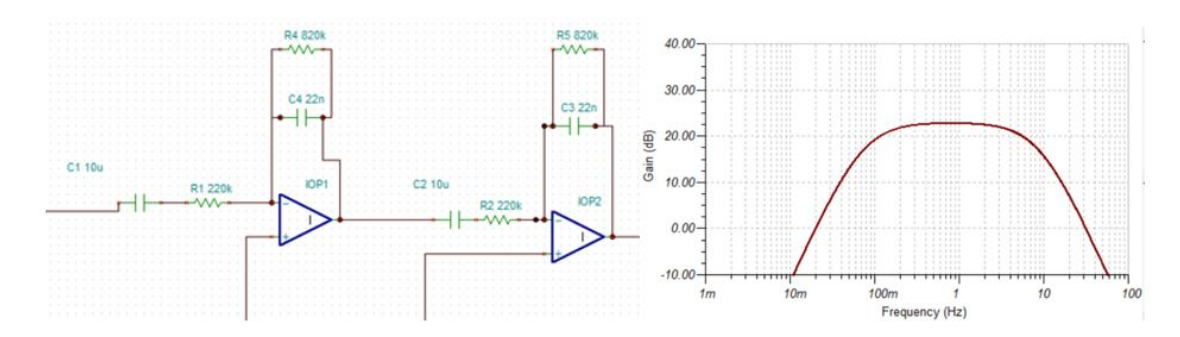


Figure 2.4 Bandpass filter response

### 2.3 Experimental Setup

The data was collected in a room measured 2.35x3.15x2.55 m and contained a bed, a chair and a table, the chair and the table were located in radar's blind spots. To select the best location for monitoring the radar, radar sensor has been tested in two different locations; the first location is on the ceiling 180 cm above the bed and the other tested location is 75 cm above the floor with a 30-degree slope to cover the floor and the bedside. A picture of the room can be seen in figure 2.5. Marks 1 and 2 show the two different tested locations of the radar. During data acquisition, only one radar sensor was operating and only one human was present in the radar field of view (the other experimenters were in different parts of the room that was not within the field of the radar).



**Figure 2.5** The setup of the experimental environment with two different radar locations

Radar's field of view is determined by the angle through which the radar could pick up reflected signals. The field of view of the utilized radar is determent by two angels: one angle of 70 degrees on the horizontal plane H-plane, and the second angle of 27 degrees on the vertical plane V-plane. Consequently, the covered area is 250 x  $100 = 25000 \ cm^2 = 2.5m^2$ , as it is shown in figure 2.6. This coverage is fine for detecting falls in the bedroom as well as the bathroom. However, for bigger rooms, like living room, depending on the area, more than one sensor or antenna might be required to cover the wider area.

In this study, the radar is placed in the bedroom in a position to cover the area near the bed. While placing the radar, radar's H-plane is set to cover the bed's width and V-plane covers the bed's length. Fall data are collected with two different heights of the bed one is 45 cm and another is 60 cm.

During fall detection experiments, the radar in location 1 showed better performance comparing to the radar placed in location 2. The reason behind this performance

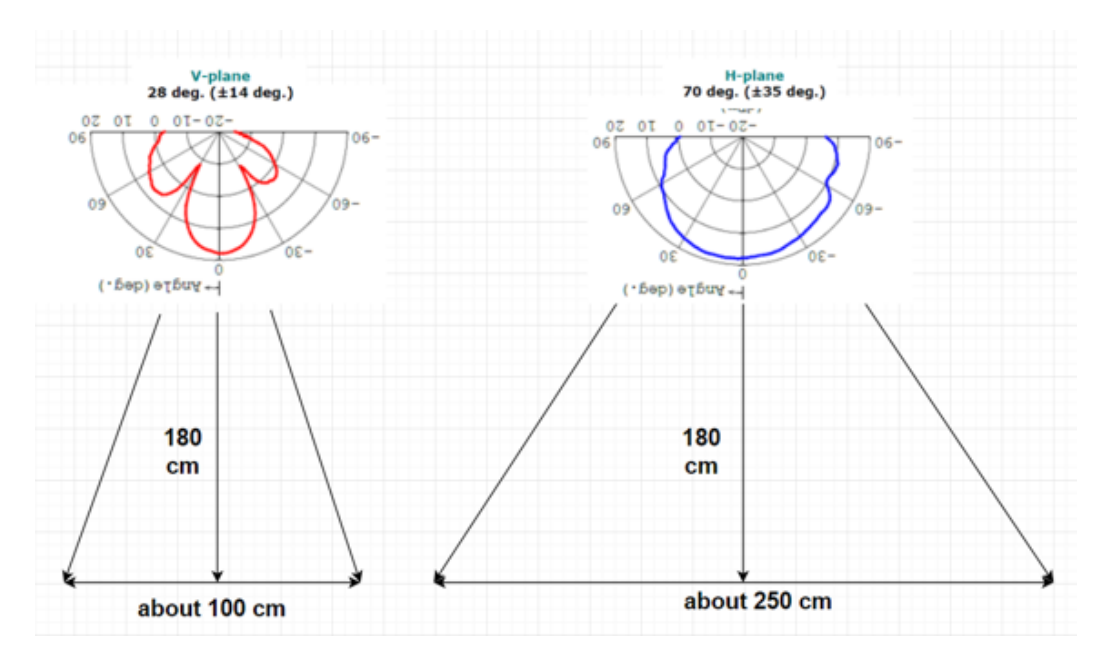


Figure 2.6 Radar's field of view

is related to the radar type which is narrow band and does not provide distance information, hence, the power of movements is influenced its distance from radar sensor. Considering this, placing the radar in location 1 guarantees that the distance from radar for all movements is within same range, is for fall detection the radar has placed in location 1, on the ceiling facing the bed. Thus, for fall detection the radar has placed in location 1, on the ceiling facing the bed.

On the other hand, for vital signs experiments, the radar sensor has been evaluated with both locations. For each radar location, two states of the subject have been tested: sitting and lying down. Considering that such project is developed for home usage purposes, daily life scenarios such as radar facing the chest, radar facing the back and radar facing the subject's side have been evaluated for each state.

### 2.4 Data Collection

Different protocols have been followed during both fall detection and vital signs measurement evaluations. During fall data collection, the fall spot is considered to be in the area near the bed onto a soft gym mattress to reduce the forces by impact to a safe level. In order to ensure that the simulated falls are typical of those experienced by older adults, Fall experiments are organized considering the fall statuses conducted by [87] as five different types: 1) falls from the bed while lying, 2) falls from the bed while sitting, 3) falls from the bed while trying to stand, 4) falls while walking to the bed, and 5) falls while trying to enter the bed. Similarly, non-fall related activities are collected considering all possible normal daily activities including siting, standing,

lying down, changing position in bed, kneeling, and picking something from the floor.

Eventually, a dataset of a total of 121 fall signatures and 117 non-fall signatures has been collected from 10 actor subjects (6 males and 4 females). Weight, high and age information of each subject is presented in table 2.1

Collected data are synchronized, segmented and saved in separate files. The digital signal is then analyzed using different signal processing techniques. Analyzing processes have been done in MATLAB 2019b environment.

Table 2.1 Participated subjects details

Subject	Gender	High	Weight	Age
S1	Male	170	70	25
S2	Male	170	83	27
S3	Female	160	50	30
S4	Female	160	50	26
S5	Male	177	71	17
S6	Male	170	58	17
S7	Male	180	55	25
S8	Male	185	55	17
S9	Female	158	48	25
S10	Female	165	60	28

Fall incidents are found to be shorter (time-wise) compared to normal body activities. The average duration of a fall is roughly 1.5 seconds, whereas, normal daily activities vary between short limb movements which last only a few seconds and walking which could last for minutes. Thus, duration of the action is regarded as an important feature to be considered for the next steps.

Initially, an evaluation of fall detection possibility with Doppler radar sensor has been analyzed. For this, three different fall scenarios are evaluated, the time domain signal of each scenario is represented in figure 2.7. The first scenario presents the signal of 30 seconds when the room is empty then a fall event, and after the fall 30 seconds when the person keeps clam on the floor and then the person stands up and leaves the room. The second scenario presents possible movements and changing positions in bed, and a fall event. Finally, the third scenario presents a fall event and continuous small random body movements such as hand, foot, and head movements. The signal sections related to fall events are the ones within the red bounders.

Then the signal response in different domains including time domain, frequency domain and time-frequency domain has been studied, figure 2.8 presents signal related to the first scenario in the time domain, frequency domain and time-frequency

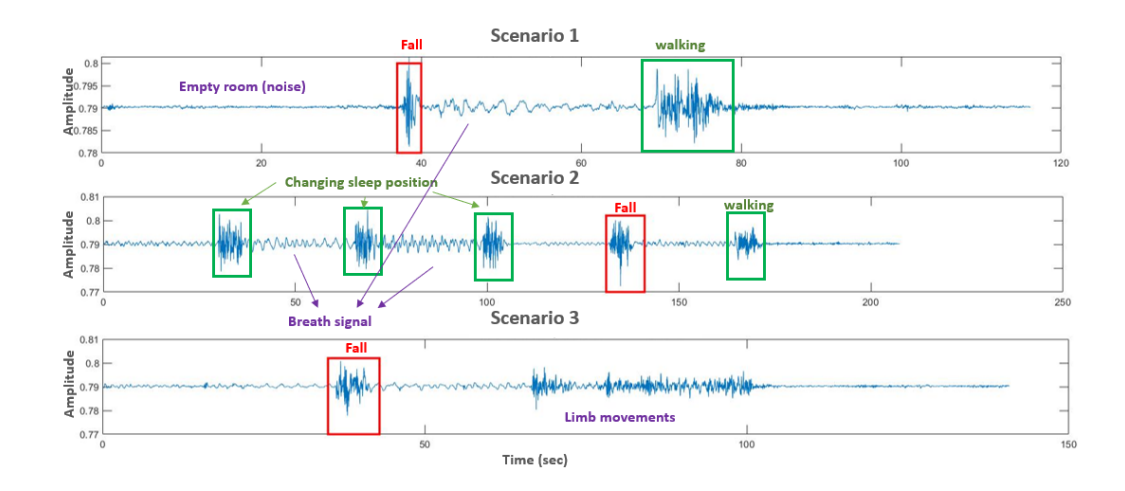


Figure 2.7 Different scenarios followed while collecting data

### power.

Our initial analysis shows that, in the time domain, fall and normal daily activities have different signatures, however, in some cases such as position changing in bed, fall and normal daily activities could have similar signatures which could cause false alarms. On the other hand, in the frequency domain, fall and normal daily activities have different signatures except for some cases when the movements are fast. These cases are evaluated even though the movements of elder seniors are more likely to be slow. A more accurate system is designed using features extracted from time and frequency domains. Extracted features are then evaluated to select the best-fit features and eliminate non-useful ones, as it is explained in the followed sections.

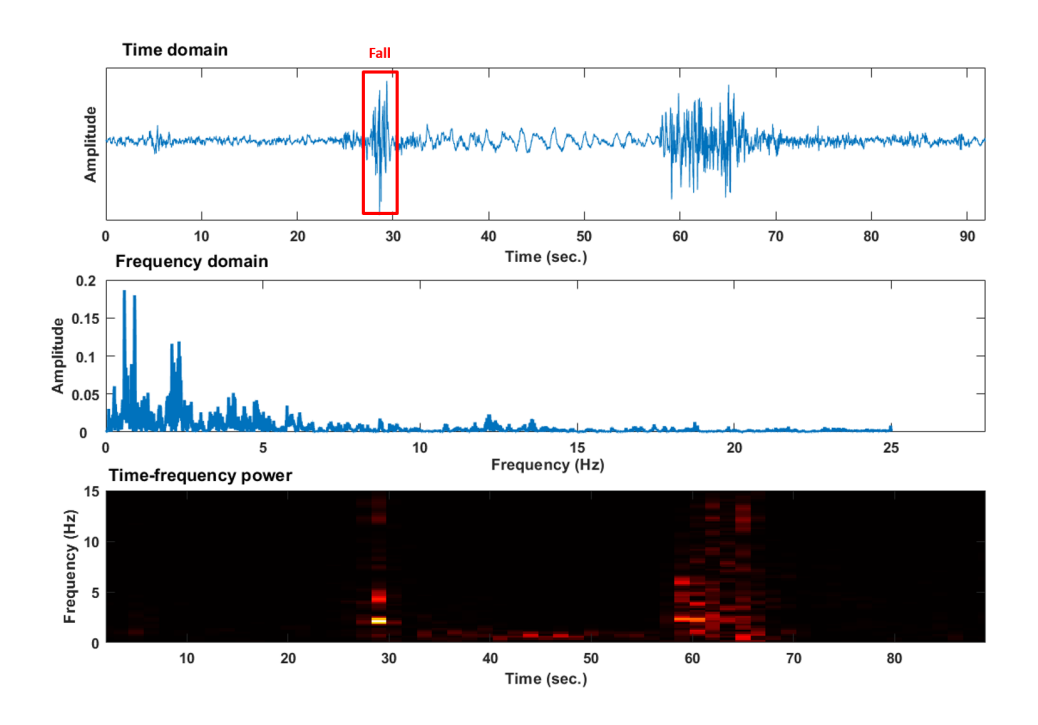


Figure 2.8 Time and frequency domains corresponded to scenario 1

# 3 METHODOLOGY

This chapter explains in detail the steps followed for completing the fall detection process. Where, the gathered signal is divided into windows and each window is: first pre-processed to remove the DC artifact and avoid the null point problem. Then, activities related to major body movements are extracted and classified to detect if it is related to a fall action or not. When a window is classified as a fall, next windows are further processed to extract and monitor the person's status and vital signs. Figure 3.1 shows the flowchart of the fall detection system presented by the sequence of the system's main steps.

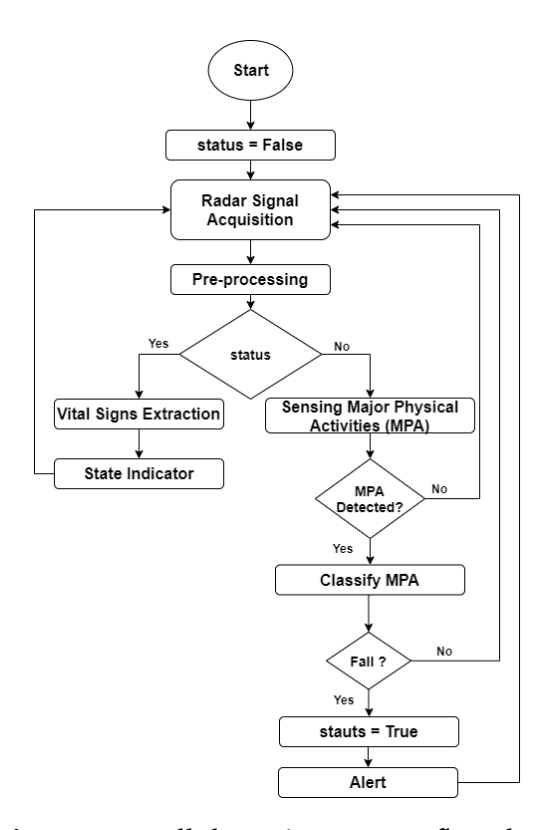


Figure 3.1 Fall detection system flowchart

### 3.1 Pre-processing

By sampling radar output signals for every 4 milliseconds, time series signals with a 250 Hz sampling rate are generated. The Arduino sketch uses Interrupt Service Routine (ISR) to accurately limit the sampling interval to 4 milliseconds (250 Hz). The signal is further divided into smaller windows with 50% overlap. The used window size in the fall detection task is 1.5 seconds-length, whereas, 30 seconds-length windows are used for vital signs extraction. Null points occur in CW Doppler radar systems when the received signal and the local oscillator are either in-phase or 180 degrees out of phase [88]. Thus, to avoid the null-point problem and calculate a more accurate estimation of displacements in the reflected wave, a more efficient combination of I(t) and Q(t) is required. For this purpose, several approaches have been proposed [89–91]. The most commonly used method is arctangent demodulation, also referred as direct phase demodulation, which is mathematically represented as in equation 3.1

$$ATAN(t) = \arctan\left(\frac{Q(t)}{I(t)}\right).$$
 (3.1)

Additionally, the static distance existed as a direct current (DC) component in the baseband signals causes a linear transform on I and Q components. For more accurate phase demodulation, DC offset is removed by extracting the mean value of each window [92].

### 3.2 Sensing Major Physical Activities

A physical activity is defined as any bodily movement produced by skeletal muscles that results in energy expenditure [93]. Major physical activities (MPA) are referred to the body movements that move the muscles and require more energy than resting. Walking, standing, sitting, lying down, and falling are examples of major physical activities. In this study, since we aim to detect fall events, MPAs are classified as fall or non-fall. Therefore, windows related to MPA are first detected and then passed to a classification model to be classified as fall or non-fall. For detecting MPAs, sliding root-mean-squared (RMS) method is used; the method basically computes the RMS value of each extracted window and compares it to a empirical threshold value. Windows that have an RMS score higher than the threshold value are detected as MPA. The RMS score for window wi is computed using equation 3.2.

$$RMS(w_i) = \sqrt{sum(w_i^2)n}$$
 (3.2)

For this study a threshold equals to 15 RMS-score is selected to be used for identifying MPAs. The RMS scores with their response to the selected threshold value following different scenarios are shown in figure 3.2.

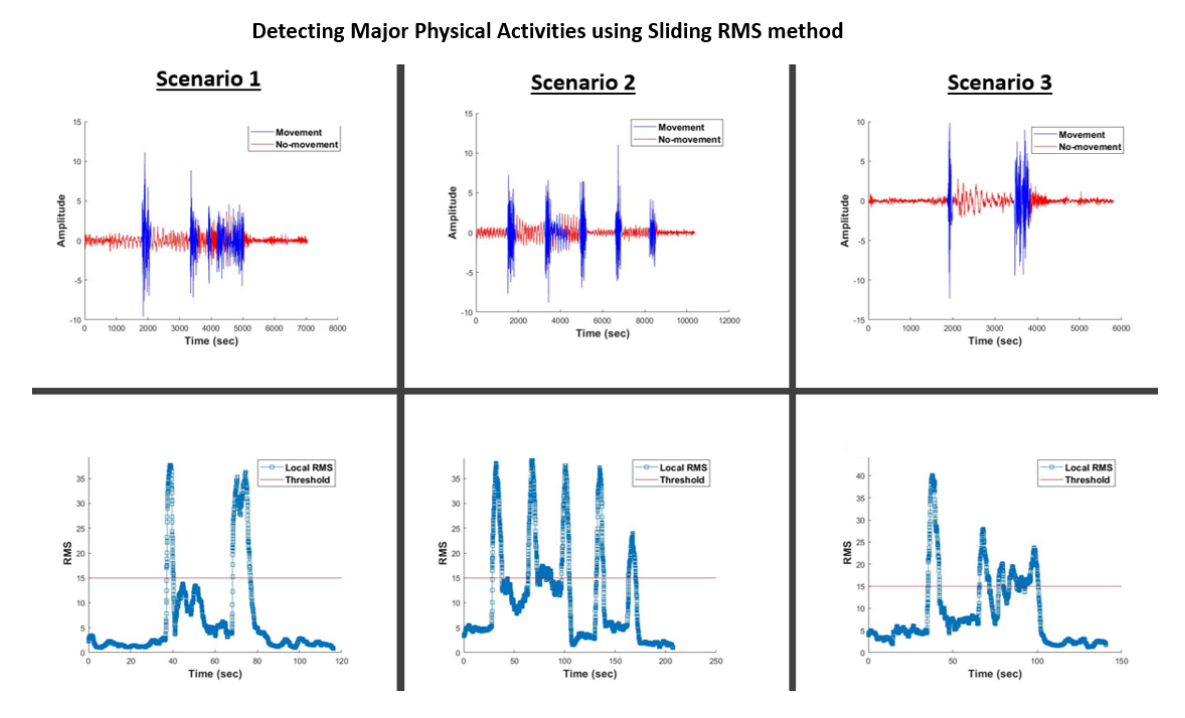


Figure 3.2 RMS scores for different scenarios

### 3.3 Fall Detection

Detected MPA is further processed to determine if it is caused by falls or other physical activities like standing or kneeling. For this step, a binary classifier has been designed based on the data collected as explained in section 2. However, designing an ideal model -that distinguishes between data related to falls and other non-fall activities and reduces the number of false alarms- requires careful selection of the applied techniques and algorithms in each step. In this section, the evaluated techniques and hipper parameters for feature engineering and classification are discussed in details.

#### 3.3.1 Features Extraction

The initial processes of the signal showed that both time patterns and frequency components contain information about the movement. Therefore, more accurate classification results require the usage of appropriate features of both classes. So, a pool of features has been extracted and then using appropriate feature selection algorithms, the critical features are selected.

#### 3.3.1.1 Time Domain Features

Studies conducted on biomedical and speech signal processing and classification in the literature have used features extracted from time domain to represent signal characteristics. After examining time features used in the literature, features extracted from the radar signal are:

• Root mean-squared (RMS) value: RMS is a commonly used feature for movement classification as it represents the average power of radar signal [94]. For radar signal x(n) with N samples RMS is calculated as:

$$RMS = \sqrt{\frac{1}{N} \sum_{n=0}^{N-1} x^2(n)}$$
 (3.3)

- Zero-crossing rate (ZCR): represents how many times the signal has crossed the zero level within a certain time window. Thus, ZRC value could be used to measure the speed of the signal [95] which makes it a suitable feature for fall activity detection -considering that falls speed is higher than other activities speeds especially for the case of elder people-.
- Turns count (TC): represents how many times the derivative of the signal has crossed the zero level within a certain time window. The advantage of TC over ZCR is that TC is not affected by low-frequency movements, artifacts and DC bias [96].
- Three Central Moments: are used to analyze the amplitude of the signal [97]. Considering a signal x(n), the k-th central moment is given by:

$$m_k = E(x - \mu)^k \tag{3.4}$$

 $\mu$  is the mean value and E(x) is the expected value. E(x) is computed by taking the time average over the duration of the . The first four central moments are evaluated as features whereas the higher order moments are considered unusual features and have been discarded for their highly sensitive to noise. Since the first moment is zero, it is also eliminated, while second moment (variance), third moment (skewness), and forth moment (kurtosis) are considered.

• Mobility (MOB): MOB is another feature used to analyse possible activities in the signal. MOB is computed as [98]:

$$M_{x} = \sqrt{\frac{\sigma_{x'}^{2}}{\sigma_{x}^{2}}} = \frac{\sigma_{x'}}{\sigma_{x}}$$
 (3.5)

here x' is the first derivative of the signal.

• Form Factor (FF): FF is also used for activity classification and it is computed as [98]:

$$FF_{x} = \frac{M_{x'}}{M_{y}} = \frac{\sigma_{x''}\sigma_{x'}}{\sigma_{y'}\sigma_{y}} \tag{3.6}$$

where x'' is the second derivative of the signal.

### 3.3.1.2 Frequency Domain Features

Since different movements contain different frequency components, extracting features from frequency domain would help in classifying and detecting the physical activities. Considered frequency domain features are:

• Four Spectral moments & two Spectral features: Power spectral density (PSD) measures the signal power at variance with its frequency. Moments of PSD have been generated and used as features. The first moment represents the mean frequency and it is calculated by [95, 99]:

$$\bar{f} = f_s \frac{2}{N_{FFT} E_x} \sum_{k=0}^{N_{FFT}/2 - 1} k S_{xx}(k)$$
 (3.7)

here fs is the sample rate (sampling frequency). Ex is the total power and is computed as:

$$E_x = \frac{1}{N_{FFT}} \sum_{k=0}^{N_{FFT}-1} |X(k)|^2$$
 (3.8)

Additionally, Median frequency - the frequency which splits PSD in half - is used as a feature and it is computed as:

$$f_{med} = \frac{m}{N_{FFT}} f_s \tag{3.9}$$

with the largest m such

$$\frac{2}{N_{FFT}E_x} \sum_{m=0}^{k=0} S_{xx}(k) < \frac{1}{2}; 0 \le m \le \frac{N_{FFT}}{2}$$
 (3.10)

The spectral moments with higher order are computed as [99]:

$$f_{mi} = f_s \frac{2}{N_{FFT} E_x} \sum_{k=0}^{N_{FFT}/2-1} (k - \bar{k})^i S_{xx}(k)$$
 (3.11)

where  $f_{mi}$  is the i-th order spectral moment and  $\bar{k}$  is the DFT sample index corresponding to mean frequency  $\bar{f}$ . The second moment is the spectral variance which represents the spectral spread in reference to the mean frequency. Third moment is spectral skewness, and the fourth moment is spectral kurtosis.

• *Spectral power fractions:* although PSD moments statistical information about the PSD, extracting special features related to previous knowledge about the signal could be helpful. Based on previous knowledge about the signal, it is observable that: in order to distinguish between signals related to different movements, different frequency features have to be analyzed for different bands separately. For this end, the spectral power fraction for a frequency band between two frequencies *f* 1 and *f* 2 is calculated as [95]:

$$E_{(f_1:f_2)} = \frac{2}{E_x} \sum_{k=k_1}^{k_2} |X(k)|^2$$
 (3.12)

here, kl and k2 are the DFT indices related to f1 and f2. Spectral power fractions are computed for two different groups separately. The first group considered six different frequency bands as:

- Band1 (0.2-0.667 Hz) covers frequencies related to breathing activities.
- Band2 (0.667-3 Hz) covers frequencies related to heart activities.
- Band3 (3-5 Hz), Band4 (5-8 Hz).
- Band5 (8-11 Hz), Band6(11-18 Hz), Band7(18-25 Hz).
- and Band8 ( $\geq$  25 Hz) covers frequencies related to different body activities.

On the other hand, the second evaluated group considered only three frequency groups as low frequencies between 0.5 Hz and 5 Hz, meddle frequencies between 5 Hz and 15 Hz, and high frequencies equal to or higher than 15 Hz.

• Spectral power ratios: The ratio between extracted power fractions is used to discriminate between signals related to different movements. The spectral power ratio between two frequency bands like (f1:f2) and (f3:f4) is calculated as [100]:

$$E_{(f_1:f_2)} = \frac{\sum_{k=k_1}^{k_2} |X(k)|^2}{\sum_{k=k_3}^{k_4} |X(k)|^2}$$
(3.13)

where kl, k2, k3, and k4 are the DFT indices for f1, f2, f3, and f4, respectively.

Extracted features are presented in table A.1 and table A.2, in appendix section. The correlation between features are presented in figure 3.3.

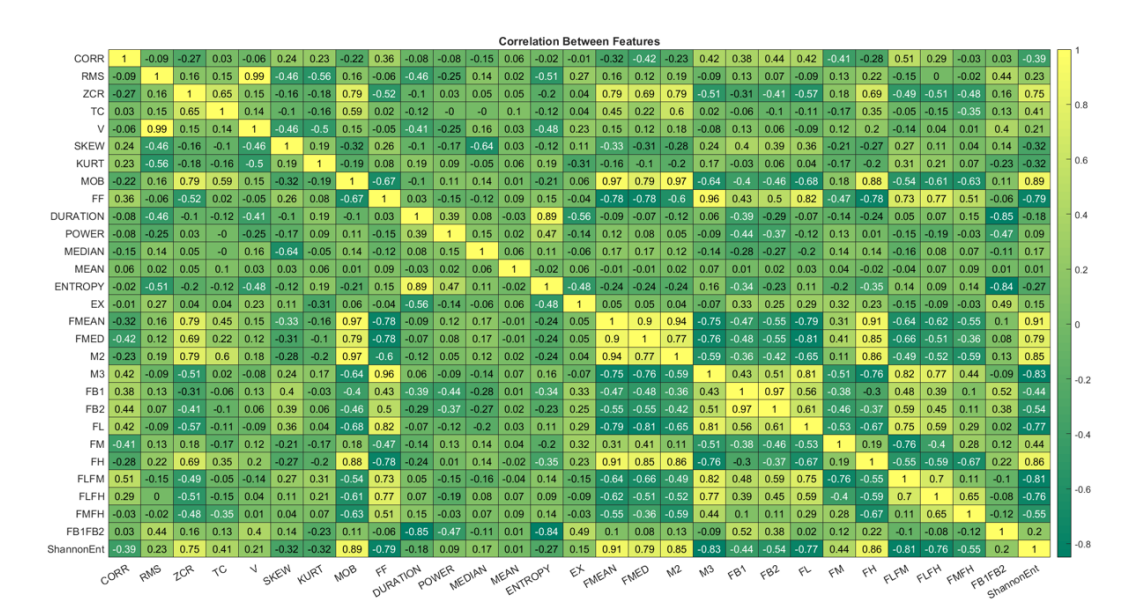


Figure 3.3 Correlation Matrix Between Features

Considering that significant correlation is when correlation scores are smaller that -0.4 or higher than 0.5, it can be seen that a large group of features have significant correlation between each other as it is shown in figure 3.4. Thus, more details about the distribution of each feature and the correlation between different feature groups is discussed in the next section.

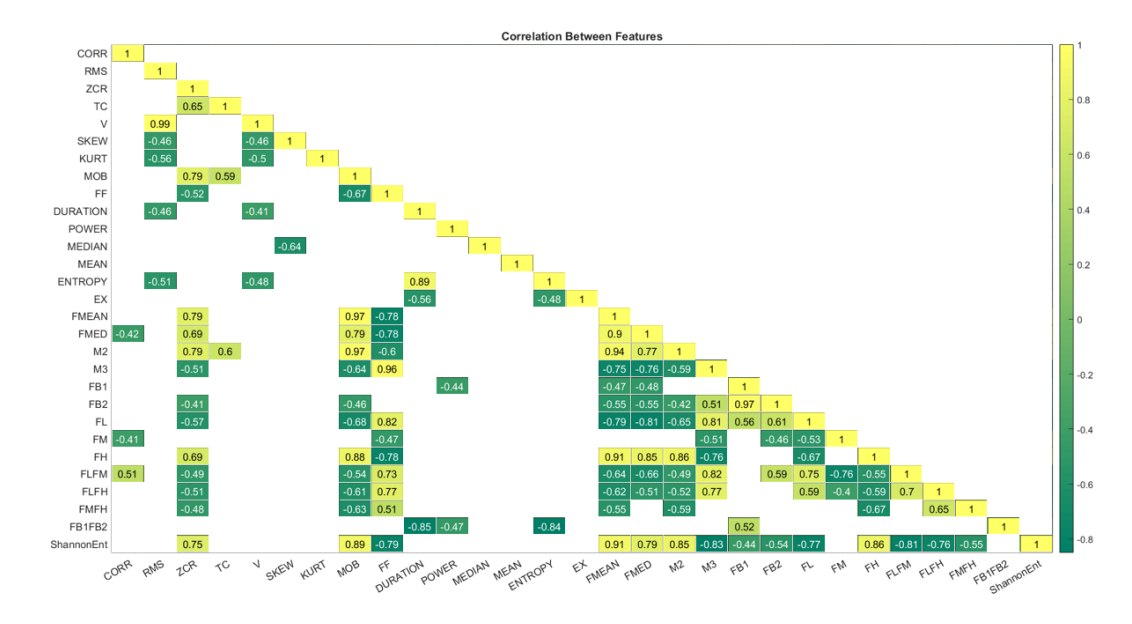


Figure 3.4 Significant Correlation Between Features

### 3.3.1.3 Correlation Between Features

To examine extracted features in more details and get better understanding of the results gathered by feature evaluating algorithms, the correlation between features

have been analyzed. Correlation represents the relationship between the features in the dataset and feature correlation is considered an important factor to be considered while selecting features. The existence of high correlated features in the dataset increases the chance that the performance of the build model will be affected by a problem referred as multicollinearity. Multicollinearity occurs when a predictor variable in a multiple regression model can be linearly generated from the others with high accuracy, which could cause skewed or misleading results. Some algorithms like decision trees and boosted trees are immune to multicollinearity, When a split feature is selected, only one of the correlated features are chosen. On the other hand, other algorithms like Linear Regression and Logistic Regression are not immune to this problem and it should be fixed before training the model. since the feature number is big visualizing the features correlation all together will present unclear view. For this reason, the correlation between features was presented in groups as: correlation between time domain features (figure 3.5) and correlation between frequency domain features (figure 3.6, figure 3.7, and figure 3.8).

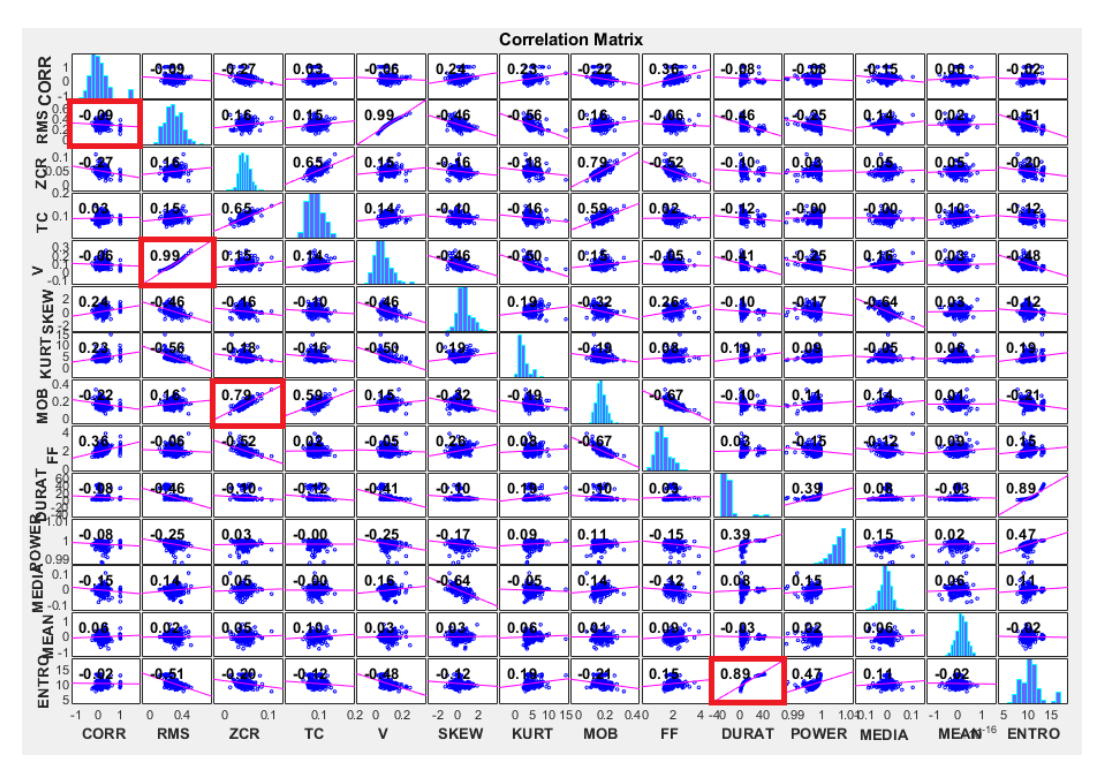
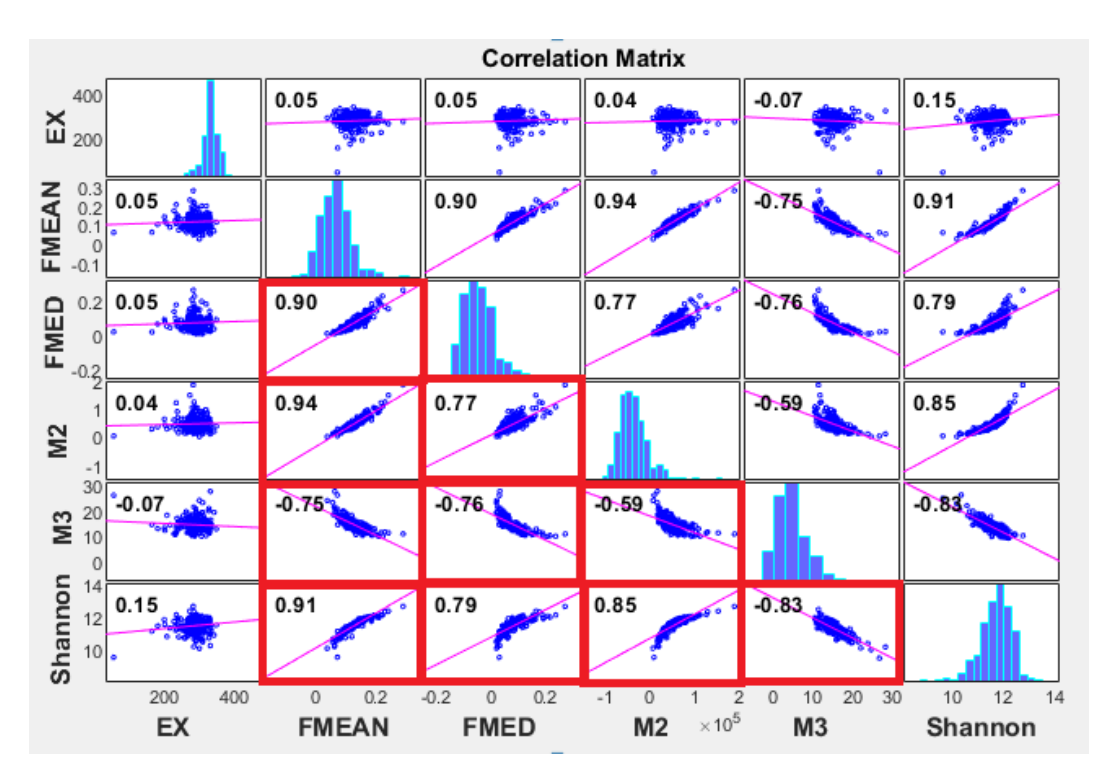
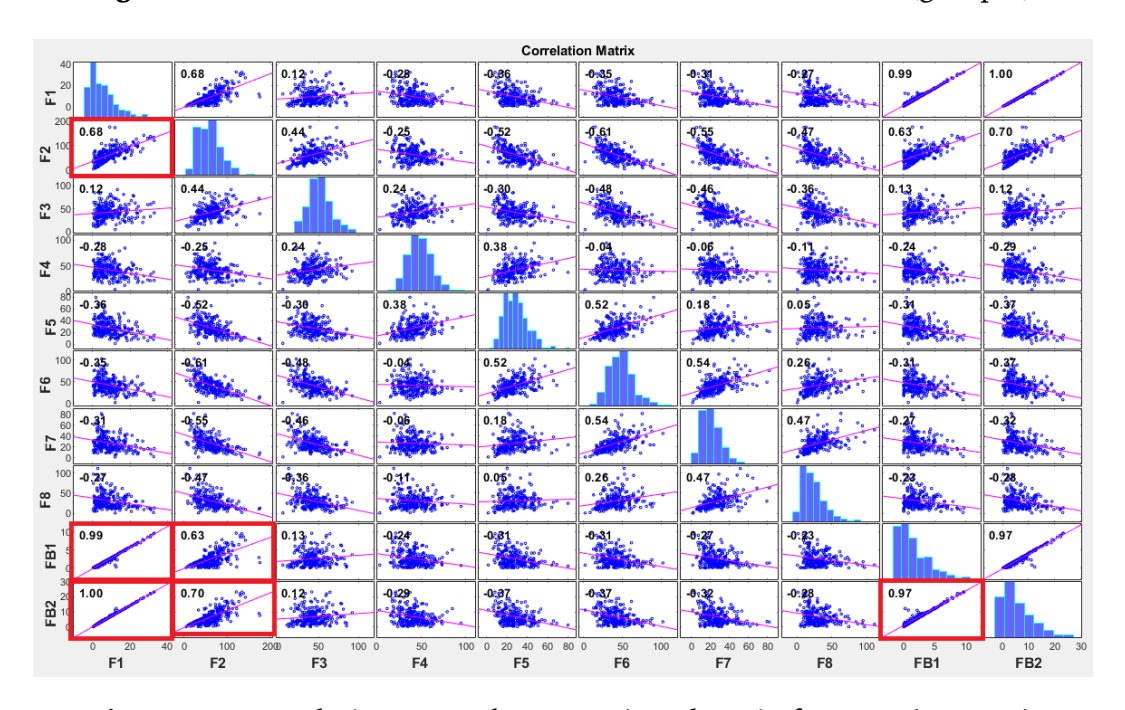


Figure 3.5 Correlation scores between time domain features

Correlation matrix between features extracted in time domain shows that ZCR and MOB, variance and RMS, and, Duration and Entropy are highly correlated to each other. On the other hand, correlation between frequency domain features shows that: FMEAN, FMED, M1, M2 and ShannonEnt all have high correlation and F1, F2, FB2 and FB1 are also highly correlated. However almost all features extracted by taking the ratio between different spectral powers are highly correlated to each other and



**Figure 3.6** Correlation scores between time domain features (group 1)



**Figure 3.7** Correlation scores between time domain features (group 2)

they could have bad effect on the dataset.

### 3.3.2 Data Visualization

59 features have been extracted as explained in the previous subsection. As first step for evaluating features, the distribution of all labeled data samples represented by

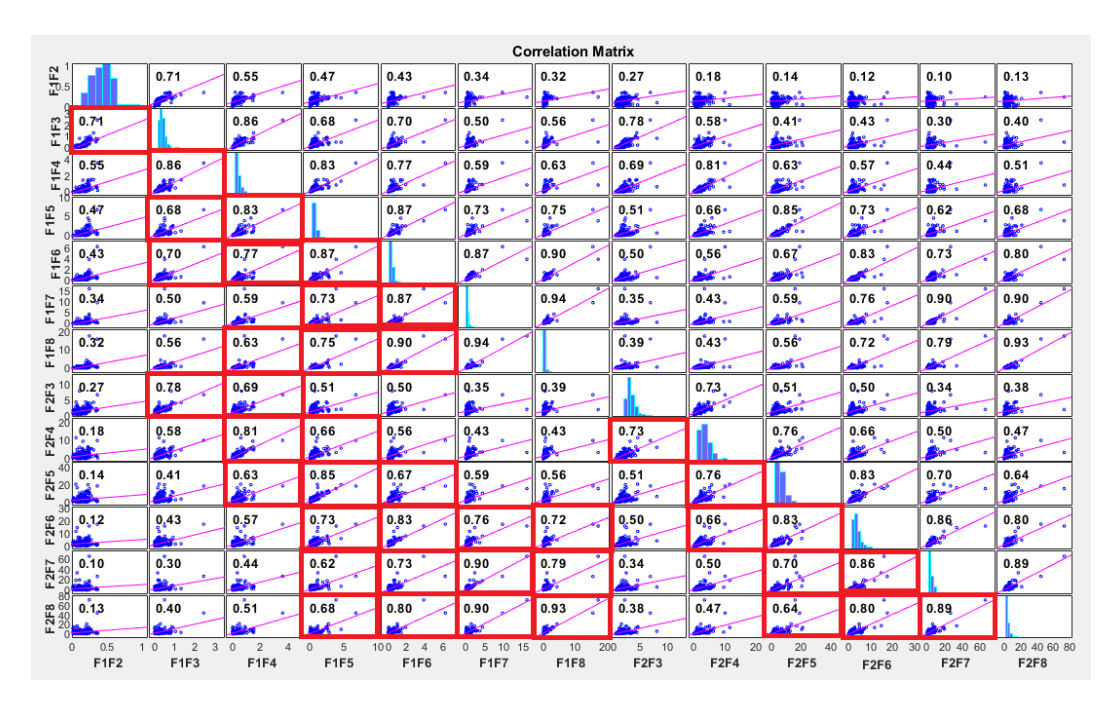


**Figure 3.8** Correlation scores between time domain features (group 3)

extracted features has been visualized. At this step, not only the distribution but also the effect of different distance parameters on the classes separation is examined. t-Distributed Stochastic Neighbor Embedding (t-SNE) technique [101] has been used for this aim. t-SNE is a non-linear technique used for dimension reduction and high-dimensional datasets visualization. The mechanism of this technique is basically based on mapping data points from the high dimensional space to a low dimensional space and finding patterns in the data by identifying clusters based on similarities between data points with multiple features. The similarity between points is calculated as the conditional probability of similarity between pairs under a normal (Gaussian) distribution. Where, a point Y is considered as a neighbor to point X if they are picked in proportion to their probability density under a normal distribution centered at X. However, after this process, the input features are no longer identifiable, and it is not possible to make any inference based on t-SNE output. Therefor t-SNE is mainly used only for data exploration and visualization.

#### 3.3.3 Feature Scaling

Before going further with feature selection and classification, feature scales should be considered and asset. Feature scaling is an important sub-step in the pre-processing step, and it could have high effect on classification results. Classification algorithms that are affected by feature scales are mostly these that computes distance or assumes normality for building classification models, like kNN and PCA. Since these algorithms only consider the magnitude of features and ignore the units while calculating

distances, features with high magnitudes will weigh more than features with low magnitudes. Subsequently, the results will greatly vary between different units. On the other hand, performing feature scaling may not have big effect in algorithms that are not distance based like tree-based algorithms, or give weights to the features accordingly like Linear Discriminant Analysis (LDA) and Naive Bayes. In this study, three different feature scaling techniques has been evaluated, examined techniques are:

• *Standardization (z-score):* replaces the values by their z-scores with mean 0 and standard deviation 1.

$$x' = \frac{x - \bar{x}}{\sigma} \tag{3.14}$$

• *Min-Max Scaling (range)*: brings the value between 0 and 1.

$$x' = \frac{x - \min(x)}{\max(x) - \min(x)}$$
 (3.15)

• *Mean Normalization (center):* this distribution will have values between -1 and 1 with  $\mu = 0$ .

$$x' = \frac{x - \operatorname{mean}(x)}{\operatorname{max}(x) - \operatorname{min}(x)}$$
(3.16)

### 3.3.4 Feature Evaluation and Selection

Reducing the number of used features is necessary for many reasons such as [102]:

- Avoid overfitting; because with datasets that contain high number of features, the built training model has perfectly fit on training samples, but it is not generalize to the new samples and relates to low accurate results.
- Develop simpler classification model; datasets with a smaller number of features deliver more simple and easy to understand models.
- Eliminate poor-quality features; having high number of features, the possibility to contain poor quality features is higher, and poor-quality features relates to build poor quality models.
- In addition, a large number of features interacts to build model which is huge, time-taking, and hard to implement in production.

A lot of machine learning techniques has been developed and improved for feature evaluating and selection purposes. In this study, considering existed techniques and the conditions for using each of them as it is mention in [103], a group of the most suitable techniques for this problem-as binary supervised with continuous features-are selected and used to evaluate extracted features. In order to consider the output of all techniques an ensemble learner has been used to calculate the final score for each feature by considering the median decision of all techniques decisions. Moreover, since the most important criteria to be considered while building an ensemble learner is to maximize the diversity between base learners, algorithms from different types with different aspects are chosen. Initially, an ensemble of five different feature selection algorithms has been developed, selected algorithms are considered to be under the three major groups of feature selection algorithms as:

- 1. Filter based methods: generally, assess the importance of the features depending on the characteristics of the data. We are more interested with filter based methods because they are independent of any learning algorithms. Algorithms we used under this type are:
  - *ReliefF*: is a similarity-based feature selection method which evaluates a feature by how well its value distinguishes the samples from different groups but are similar to each other. For each feature f, ReliefF selects a random sample and its k nearest neighbors from same class and each of different classes. Then the sum of weighted differences in different classes and the same class is calculated. If f is deferentially expressed, differences for samples from different classes will be greater and f will has higher score (and vice versa) [5].
  - Mutual Information Maximization (İnformation Gain): is an information theory-based method that evaluates a feature by its correlation with the class labels, as it is built on the assumption that a strong correlation between the features and the class labels helps to achieve good classification performance.
  - *T-score:* is a statistical-based method especially used for binary classification methods. The main idea of this method is to compute the ratio between the variance and the mean difference between two classes for a feature and assess whether it makes the means of the two classes statistically different.
  - Bhattacharyya Distance: measures the separation between two classes distribution, it computes the distance between classes defined by related features. Higher Bhattacharyya distance indicates less overlapped and better-separated distributions of classes. Meanwhile, when two classes have exactly the same distributions, the Bhattacharyya distance is zero.

In [104], the relationship between Bayes error and Bhattacharyya distance is studied and it has been found that a Bhattacharyya distance higher than 0.8 guaranty a classification error less than 10%.

- 2. Wrapper-based methods: evaluates the features according to their effect on the performance of predefined leaning algorithm. Methods from this category are not used at this step since we do not have a target learning algorithm and testing with different learning algorithms will complicate the evaluation step. However, in the next step, at the final decision for the selected features, a similar approach is followed.
- 3. Embedded methods: basically, relays on using algorithms which have built-in feature selection methods, and the output of these algorithms when there are used for feature evaluation in most cases is in as used or not-used. For this study, we used Random Forest (RF) algorithm to evaluate the importance of features from embedded perspective.

The general flowchart for feature evaluation steps is shown in figure 3.9.

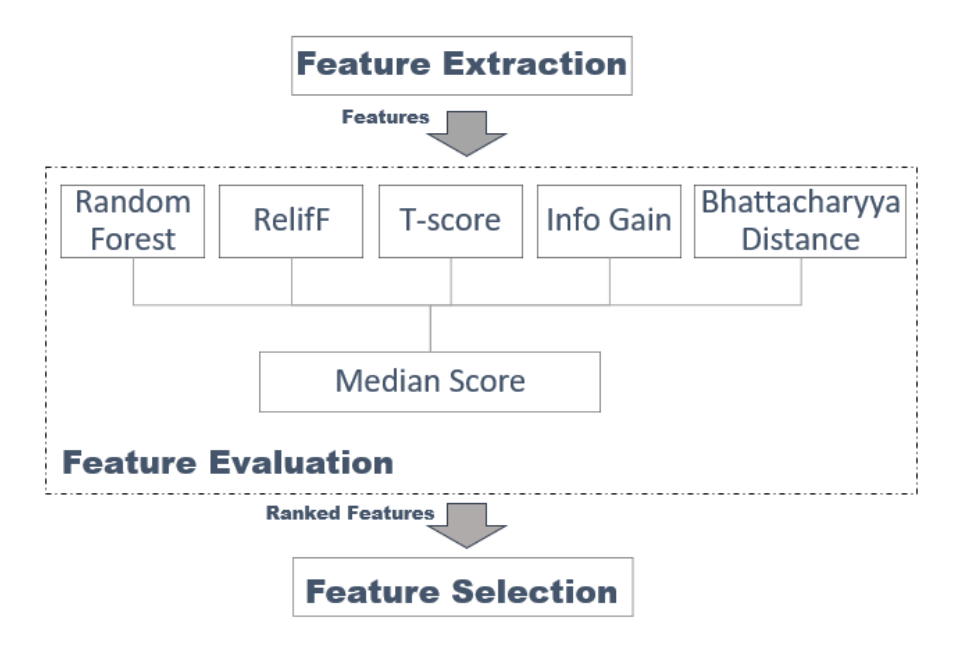


Figure 3.9 Main steps followed for feature engineering

### 3.3.5 Designing Classification Model

While developing a classification model, two phases are involved: training phase and test phase. In the training phase the classification model is build using labeled data and this model is used later to classify new samples. Two important parameters are discussed in this section: the data used for training the model and the classification algorithm used to build the model.

### 3.3.5.1 Train, Validation and Test sets

To build a classification model, the used dataset is usually split into two subsets called as train set and test set. Train set contain labeled data that are used to build the classification model which is then used to make predictions on the test set. The percentage of train set over test set is usually selected as 80/20, 70/30 or 60/40. By using only train and test sets, the algorithm tries to generate the perfect build-in model. However, in the case when the data set has too many or too less features, classification model will have a problem called overfit in the case of too many features and underfitting in the case of too less features. Additionally, the split of train and test sets could not be fair enough and some groups of data could be only in test set and not in the train set, and by this, this built model will work good with the train set but it will be not generalized to fit the test set and will not recognize samples belong to the missed group which leads to poor classification performance and low accuracy results. Anyhow, by splitting the dataset into three subsets: train, validate and test sets and using cross validation (CV) technique will avoid such problems and guarantee building more generalized model. Basically, CV is repeating to the classic train test step more than one time, each time different data samples are used for the train and test, and then the best fit model is selected as the final model. There are different methods of CV, in this work k-fold CV is used. In k-fold CV, the train set is split to k subsets called folds, then k-1 subsets are used to build the model and one subset is used to test that model. This is repeated till all subsets are used as test set. By the end of this step, k classification models will be built, the average of these models is then taken to generate the final model. Finally, the performance of the final model is evaluated using the test set. However, the number of the used folds should be carefully chosen to suit the used dataset. Although, using more folds reduces the error due to bias, it increases the error due to variance and also increases computational time and memory. Thus, usually for big datasets, a smaller number of folds, whereas, higher number of folds is used with small datasets [105]. In this study, the dataset is randomly split as 80% for train set and 20% for test set. Then, to build classification mode 5-fold CV is applied over the train set, and finally, the model accuracy is evaluated according to the model's predictions on the test set.

### 3.3.5.2 Classification Algorithms

In this section a short explanation about the classification algorithms that have been evaluated to build the most accurate model for fall detection. Since these algorithms are considered well known and widely used techniques, only a brief explanation about the algorithm, the reason for selecting it, and the implementation details are provided. However, [106] and [107] studies could be reviewed for more details and technical

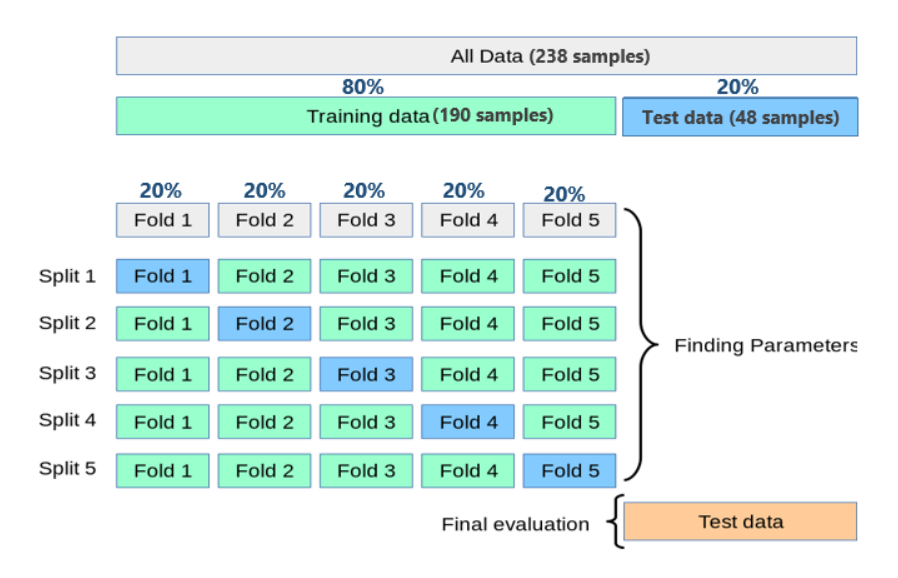


Figure 3.10 5 fold cross validation data sets separation

explanations about the algorithms.

- *Decision Tree (DT)*: is a decision support tool that presents non-linear relationships based on conditional control statements. It is considered as one of the most used supervised learning techniques. A full DT which fits the train set perfectly could produce overfitted model with low performance over the test set. To avoid overfitting the designed tree is 'curvature' technique is used, the tree stops splitting nodes if all tests yield p-value greater than 0.05. For generating DT, MATLAB function fitctree is used with 5-fold cross validation and 'curvature' method.
- Support Vector Machine (SVM): is a supervised machine learning technique that is used for both classification and regression problems. It basically, classifying data points by computing a hyperplane in an N-dimensional space that distinctly different classes. SVM model represents the samples as points in space, mapped so that the samples of different classes are divided by a gap that is as wide as possible. New examples are then mapped into the same space and predicted to belong to a class based on which side of the gap they are located. SVM builds a non-probabilistic binary linear model for binary problems, besides it performs a non-linear classification using the kernel trick, implicitly by mapping their inputs into high-dimensional feature spaces. In this project, linear SVM model has been built with 5-fold cross validation.
- *K-nearest neighbors (KNN):* is a supervised machine learning algorithm that is used for both classification and regression problems. It is a simple and easy-to-implement algorithm with the assumption that similar things are near to

each other. This algorithm does not have a training phase and to classify a new sample, the distance between this sample and the whole samples in the train set is computed, and then the mode of the labels of the nearest k samples is selected as the label of the new sample. There is no fix number of neighbors (k) to be used for the evaluation and it is totally related to the used dataset. For this reason, in this study, since the exact number of k is unknown, while comparing kNN to other algorithms, the algorithm has been evaluated which three different values of k (1,3,5).

- *Naive Bayes (NB)*: is a supervised machine learning algorithm used for classification problems. NB is based on Bayes' Theorem that assumes that features are independent among each other. One of the advantages for using NB is that it is fast, and it could be used for making predictions in real time. Thus, its performance was evaluated and compared to the other classifiers.
- *Linear Discriminant Analysis (LDA):* is a dimension reduction technique which is mostly used for the supervised classification problems. It is used for modeling samples and separating them to two or more classes, and it also projects the features in higher dimension space to lower dimension space.

### 3.4 Vital Signs Extraction

In the case when a fall is detected, the status of the fallen person is observed by monitoring his/her vital signs. In vital signs extraction stage, the signal is divided into 30 seconds-length windows with 50% overlap. First, each window is pre-processed to remove the DC artifact and avoid the null point problem. Then, noise and artifacts are filtered. Finally, heartbeat and respiration signals are extracted. Processing details are explained as the following:

#### 3.4.1 Eliminating Noise and Artifacts

Minor physical activities such as tossing, turning, trying to stand after fall, and involuntary limb movements are important information to be used for evaluating the status of the person after a fall is detected. However, such activities effect the signal by increasing its variance and power, so they are considered as noise in the vital signs extraction step, because vital signs signal contain less power.

Thus, to improve the accuracy of vital signs predictions, noise generated from random minor physical activities and noise generated by electronics artifacts is eliminated.

For this purpose, an adaptive threshold method is developed. First, for each window,

two local thresholds are calculated to generate a boundary in which only vital signals could be located. The thresholds are calculated as: mean(window) + 3\*Std (window) for the upper limit and mean(window) - 3\*Std (window) for lower limit. Then, data samples or epochs that are out of the determined range, bigger or smaller than the threshold, are considered as artifacts and removed from the signal. Finally, a linear interpolation is applied to up-sample the signal and fill the gaps caused by extracting data points with new predicted ones. This step is completed using MATLAB *gridded-Interpolant* method. Algorithm in figure 3.11 presents the main steps of the applied algorithm.

```
Algorithm 1 Noise and Artefacts Eliminating Algorithm

Inputs:
\mathcal{X} = \{x_1, x_2, \dots, x_n\} \ \text{time series window *} \ \text{``betect Outliers *} \ \text{``threshold}_1 = mean(\mathcal{X}) + 3 * \sigma(\mathcal{X}) \ \text{``threshold}_2 = mean(\mathcal{X}) - 3 * \sigma(\mathcal{X}) \ \text{``stor all } x_i \in \mathcal{X} \text{ do} \ \text{``if } x_i > threshold_1 \text{ OR } x_i < threshold_2 \text{ then} \ \text{``if } x_i = Interpolate(x_i, \mathcal{X}) \ \text{``end for} \ \text{``end for} \ \text{``spline Interpolation method is used to interpolate Detected Outliers*} \ \text{``spline Interpolation method is used to interpolate Detected Outliers*} \ \text{``spline Interpolation method is used to interpolate Detected Outliers*} \ \text{``spline Interpolation method is used to interpolate Detected Outliers*} \ \text{``spline Interpolation method is used to interpolate Detected Outliers*} \ \text{``spline Interpolation method is used to interpolate Detected Outliers*} \ \text{``spline Interpolation method is used to interpolate Detected Outliers*} \ \text{``spline Interpolation method is used to interpolate Detected Outliers*} \ \text{``spline Interpolation method is used to interpolate Detected Outliers*} \ \text{``spline Interpolate Detected Outliers} \ \text{``spline Interpolate Detected Outliers} \ \text{``spline Interpolate Detected Outliers} \ \text{``spline Interpolate Detected Outliers} \ \text{``spline Interpolate Detected Outliers} \ \text{``spline Interpolate Detected Outliers} \ \text{``spline Interpolate Detected Outliers} \ \text{``spline Interpolate Detected Outliers} \ \text{``spline Interpolate Detected Outliers} \ \text{``spline Interpolate Detected Outliers} \ \text{``spline Interpolate Detected Outliers} \ \text{``spline Interpolate Detected Outliers} \ \text{``spline Interpolate Detected Outliers} \ \text{``spline Interpolate Detected Outliers} \ \text{``spline Interpolate Detected Outliers} \ \text{``spline Interpolate Detected Outliers} \ \text{``spline Interpolate Detected Outliers} \ \text{``spline Interpolate Detected Outliers} \ \text{``spline Interpolate Detected Outliers} \ \text{``spline Interpolate Detected Outliers} \ \text{``spline Interpolate Detected Outliers} \ \text{``spline Interpolate D
```

Figure 3.11 Noise and artefacts eliminating algorithm

Figure 3.12 presents The difference between demodulated signal before and after artifact cancellation in the time domain for 3.5 minutes window.

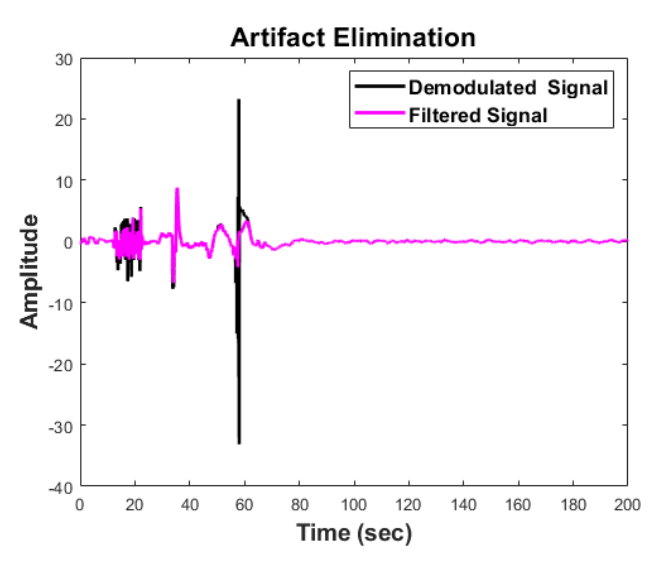


Figure 3.12 Demodulated signal before and after artifact cancellation

### 3.4.2 Heart and Respiration Rates Extraction

Two finite impulse response (FIR) bandpass filters are designed using Planck-taper window with length of 30 second and 0.1 edge decay. Planck-taper window coefficients are given by [108]:

$$a(k) = \begin{cases} 0 & k = 0\\ \frac{1}{(e^{z}a^{k}+1)} & 0 < k < \epsilon(N-1)\\ 1 & \epsilon(N-1) \le k \le (1-\epsilon)(N-1)\\ \frac{1}{(e^{z}b^{k}+1)} & (1-\epsilon)(N-1) < k < (N-1)\\ 0 & k = N-1 \end{cases}$$
(3.17)

$$z_a(k) = \epsilon (N-1) \left( \frac{1}{k} + \frac{1}{k - \epsilon(N-1)} \right)$$
(3.18)

$$z_b(k) = \epsilon (N-1) \left( \frac{1}{N-1-k} + \frac{1}{(1-\epsilon)(N-1)-k} \right)$$
 (3.19)

Where N is the length of the filter,  $0 < \epsilon \le 0.5$ , is the edge decay which controls the size of the top portion of the window, and k = 0, 1, ..., N - 1.

Since all possible values for heartbeats are between 45 and 150 cycles/min and for respirations are between 9 and 24 cycles/min, the frequency bands are selected as [0.7,2.5] for the heartbeat, and [0.1,0.5] for respiration. Figure 3.13 presents designed filter response for heartbeat signal extraction on the left, and the filter response for respiration signal extraction on the right.

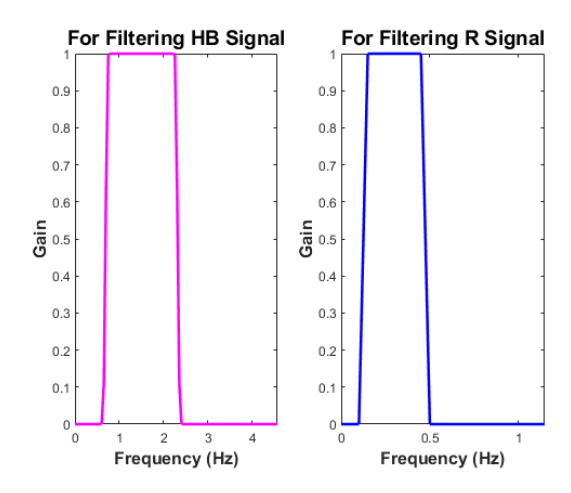


Figure 3.13 Frequency domain response of the used FIR bandpass filters

After identifying and replacing epochs with noise and body movements, the remaining

epochs are processed to extract the respiratory and heart rates. The signal is examined in 30 seconds length windows. A moving window with 30 seconds length and 15 second overlap is used. Each window is passed throw two algorithms with different parameters. One for extracting respiration signal and another is for extraction heartbeat signal. A time domain comparation between reference signal (above) and extracted respiration signal (bellow) is shown in figure 3.14-(a) Similarly, reference and extracted heartbeat signals are shown in Figure 3.14-(b).

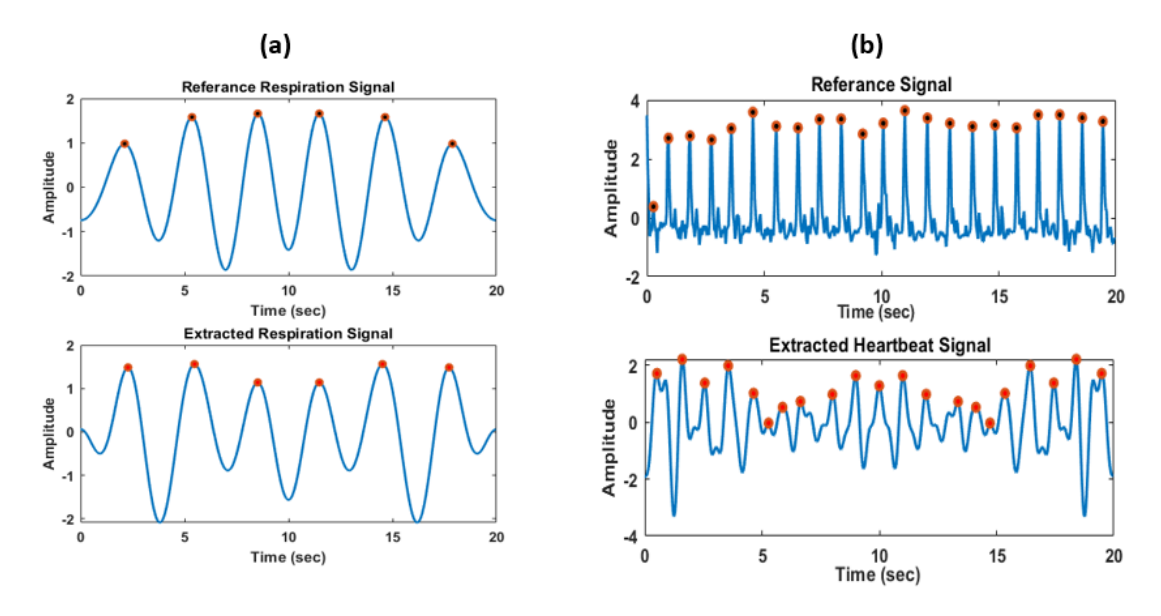


Figure 3.14 Extracted and reference signals

#### 3.4.3 Reference Sensors

To validate the efficiency of this work, two additional biometric sensors are used to compare their results with our developed algorithms' results. Both reference sensors are sampled with a single Arduino with the same sample rate as the radar (40 milliseconds / 25 Hz).

- Breath rate reference data: By means of piezoelectric sensor —a device that uses the piezoelectric effect to measure changes in pressure, acceleration, temperature, strain, or force by converting them to electrical charges, shown in Figure 3.15-(a)—the pressure caused by chest movement during breathing is measured. Then, the signal is synchronized with the radars signal and divided into windows with same length.
- *Heart rate reference data:* Pulse Sensor is used to get reference heart rate data. The Pulse Sensor is low-cost optical heart rate sensor (PPG) for Arduino and other microcontrollers [109]. Pulse Sensor has spot pressure which gives a live

clean heartbeat waveform shown in figure 3.15-(b). Then, simply, by counting peaks we get the heart beats.

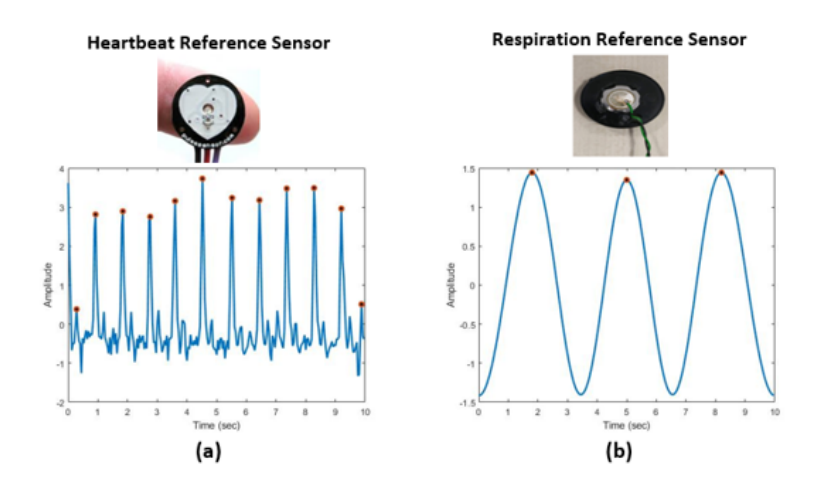


Figure 3.15 HR and RR reference sensors and signals

4

### **RESULTS and DISCUSSION**

In this chapter, the key experimental results for both vital signs monitoring and fall detection are set out, examined, and evaluated.

### 4.1 Vital Signs Monitoring

In order to make the system more robust, experiments are performed according to different daily life scenarios such as sitting, standing, laying down and sleeping, considering different positions of the subject including front, back and side. However the best results are taken when the system is facing the subject's chest with no major body movements which is considered the most likely case after fall. The distance between the system and the subject is set in range up to 2 meters.

A total of 100 minutes of recordings from 10 healthy subjects (6 males and 4 females) were used to validate the proposed system and its ability to measure vital signs rates. During experiments, radar has been located in two different locations: first location is on the ceiling with 180 cm height from the floor. Second location is on the chest level toward the subject. For each radar location, two states of the subject have been tested: sitting and lying down. Considering that such project is developed for home usage purposes, daily life scenarios such as radar facing the chest, radar facing the back and radar facing the subject's side have been evaluated for each state. Absolute mean error and accuracy percentage are used to evaluate the methods' performances. Accuracy percentage is basically calculated by measuring the closeness between predicted rates and the rates measured using reference sensors mathematically shown by equation 4.1.

$$Accuracy = \frac{HR_{ref} - \left| HR_{ref} - HR_{Radar} \right|}{HR_{ref}} \times 100(\%) \tag{4.1}$$

whereas Mean Absolute Error (MAE), simply finds the absolute difference between

predicted and actual rates, and then finds the mean of all errors, as it is in equation 4.2.

$$MAE = \frac{1}{n} \sum_{j=1}^{n} |y_j - \hat{y}_j|$$
 (4.2)

This method is suitable for evaluating results, since foe vital signs rates, less predictions and more predictions have similar effects. By comparing the system results to highly accurate biometric sensors, the proposed system achieves 97.7 accuracy for respiration detection and 95.3 accuracy for heartbeat detection with the best scenario case when the radar is facing a siting subject's chest. Achieved error and accuracy values for different measurement sets are presented in Table 4.1.

<b>Table 4.1</b> MAE and Accura	y results for different test sets
---------------------------------	-----------------------------------

Radar	Subject	Radar	Respiration		Radar   Respiration   Heartbea		tbeat
position	state	heading	Ra	Rate		ite	
			MAE	Acc	MAE	Acc	
Ceiling	Sitting	Head	3.5	82.7	13	81.7	
	Lying down	Chest	2.2	90.7	3.3	94.8	
		Back	2.7	84.8	3.1	95.8	
		Side	2.6	85.6	2.3	95.6	
Chest level	Sitting	Chest	0.8	97.7	2.5	95.3	
		Back	2.8	85.5	6.8	92.1	
		Side	2.5	87.3	4.5	94.6	
	Lying down	Chest	2.1	90.7	3.3	94.4	
		Back	2.4	89.1	7.2	88.7	
		Side	2.3	87.0	6.1	88.9	
Average			2.39	88.11	4.76	92.2	

### 4.2 Activity Classification and Fall Detection

For fall detection task; CW Doppler radar sensor-based system was developed and used to collect 121 fall and 117 non-fall signatures from 10 actor subjects. These collected signatures are referred as raw data. Then, total 59 features are then extracted from the raw data and labelled as binary problem by Fall vs non-Fall ('1' vs '0'). As a result, a dataset with 238 samples and 60 features has been generated. Total generated data samples are visualized using t-SNE technique by calculating Gaussian kernel using squared pairwise distances with four different distance metrics as it is shown in figure 4.1. The used four metrices are: Euclidean, chebychev (the maximum coordinate

difference), mahalanobis (computed using the positive definite covariance matrix), and cosine (1 – the cosine of the included angle between observations).

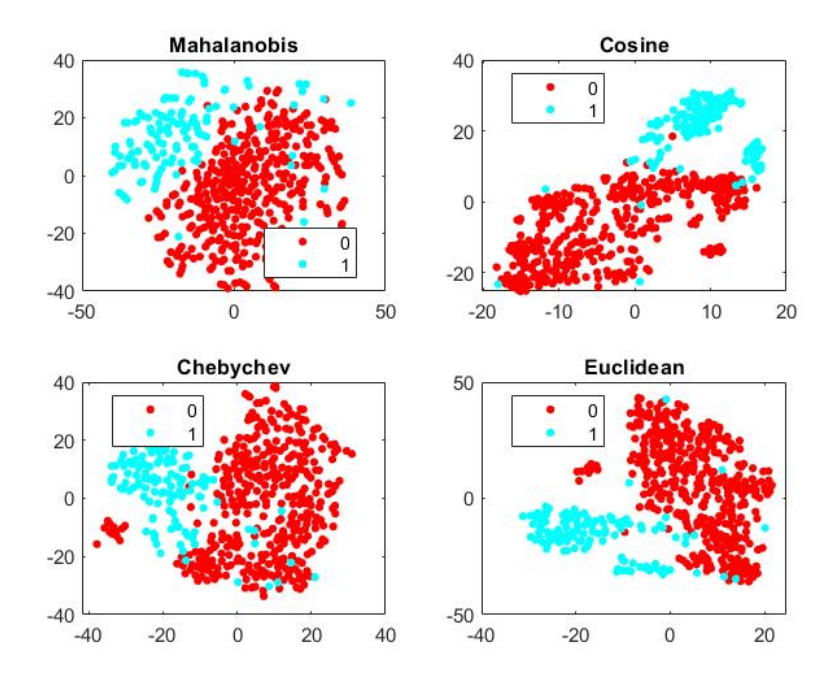


Figure 4.1 Visualization of feature distribution using different metrics

Observably, extracted features presents good distinguishing between fall and non-fall classes, and all four distance metrics have similar effect on data distribution, so, for distance based classification algorithms any one of these metrics could be used. However, for this work, Euclidean distance is selected. Although extracted features do not vary in scales, the effect of different feature scaling algorithms has been examined. The performance of different feature scaling algorithms is evaluated by comparing the results of different learning methods on the normalized datasets. Evaluated feature scaling methods are: z-score, Min-Max, and mean, whereas, considered learning methods are: DT, SVM, NB, and kNN with three different k values (1,3,5). Evaluating results are presented in figure 4.2

Results in figure 4.2 shows that normalizing the features did not effect the accuracy of the non-linear algorithms (DT and NB). Also, accuracy results of NB algorithm are same in all cases because it is based on computing probabilities between data samples, and changing the scale range dose not effect the probability results. Whereas, scaling algorithms have big effect on linear algorithms like SVM and kNN. However, Min-Max scaling algorithm is providing the best results for all algorithms, thus, before building the classification model, the data set scale is changed according to Min-Max scaling method.

To reduce the number of features and select only useful ones for building a

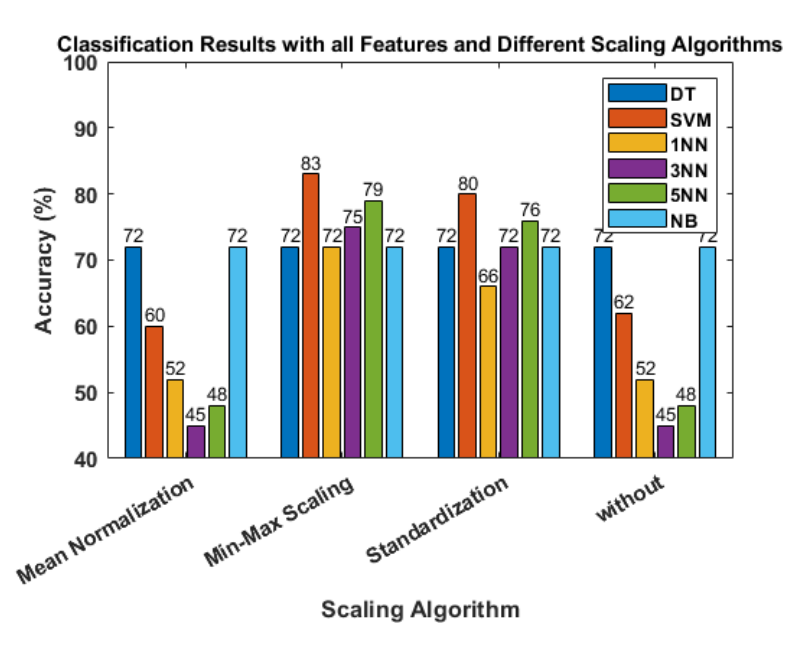


Figure 4.2 Classification Results with all Features and Different Scaling Algorithms

classification model, features are evaluated and scored by an ensemble of five different feature selection algorithms. At the first step of feature evaluation, one of the two SPF groups is eliminated. Eliminating decision is taken by comparing the performance of different classifiers on two datasets; 1) dataset1: contains SPF1(has 60 features), and 2) dataset2: contains SPF2 (has 30 features). Classifiers provided higher performance results on dataset2 as it is presented in figure 4.3. Moreover, SPF1 features are highly correlated to each other and has the lowest evaluation scores as it shown in figure 3.8.

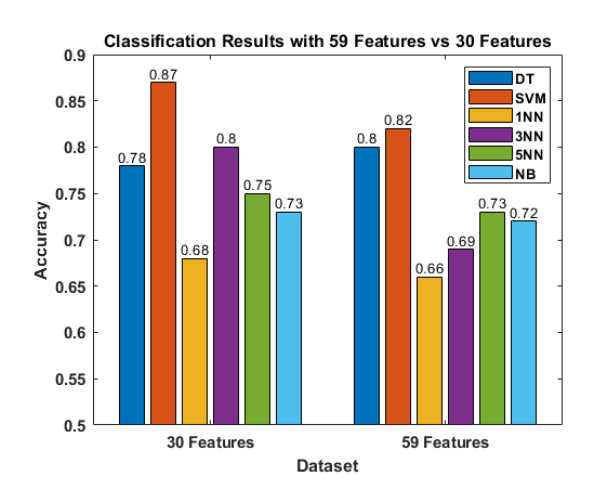


Figure 4.3 Classification results for different feature groups

Results in figure 4.3 shows that removing features related to spectral power ratios has highly improved the accuracy results of SVM, kNN and NB algorithms, whereas, the accuracy of DT has decreased by 2%. The reason behind this is that DT algorithm is immune to Multicollinearity and it choose the best correlated feature to be used and discard the rest, where other algorithms are not immune to Multicollinearity and

their accuracies have increased by removing correlated features. Even though, some algorithms like DT are not affected by correlated and low-quality features, eliminating those features still has the advantage of building simpler and more understandable model. Moreover, producing a smaller number of features and running less complex model is considered a big advantage for real time impeded systems whence saving time and memory. Thus, SPF1 is eliminated at this step while SPF2 is kept to be used for the next evaluations.

Then, for selecting the best feature subset, the features are sorted according to their importance from the most significant feature to the less significant one. The importance of each feature is presented by its final score which is the median of all given ranks by the five feature selecting algorithms. Table 4.2 presents the scores given by each algorithm to each feature, and the final score for each feature that has been used to decide the importance of each feature, lower score indicates higher importance, and vice versa. Finally, features are sorted according to their importance where the first feature represents the most important feature and second feature is the second important one and so on.

							A
		Fea	ature Evalua	nting Algorithms			
Sorted Features	Random Forest	ReliefF	T-score	Info Gain	Bhattacharyya Distance	Score (median)	Final Rank
ENTROPY	TRUE	25	1	1	5	3	1
POWER	TRUE	6	2	4	16	5	2
DURATION	TRUE	7	5	2	12	6	3
FB1FB2	TRUE	1	13	3	27	8	4
EX	TRUE	28	4	9	10	9.5	5
ZCR	FALSE	10	10	10	11	10	6
FB1	TRUE	2	16	6	19	11	7
МОВ	FALSE	14	11	12	4	11.5	8
FB2	TRUE	5	17	8	20	12.5	9
MEDIAN	TRUE	19	24	7	8	13.5	10
SKEW	TRUE	23	6	5	24	14.5	11
KURT	FALSE	20	15	14	15	15	12
FL	FALSE	11	19	26	1	15	13
FLFM	FALSE	3	23	21	9	15	14
FM	FALSE	8	22	25	7	15	15
CORR	FALSE	18	14	29	13	16	16
RMS	FALSE	15	28	11	18	16.5	17
MEAN	FALSE	27	7	17	17	17	18
M3	FALSE	4	9	28	26	17.5	19
v	FALSE	21	21	15	3	18	20
FLFH	FALSE	16	8	20	29	18	21
FH	FALSE	13	26	23	14	18.5	22
FF	FALSE	24	12	16	23	19.5	23
FMED	FALSE	9	18	24	21	19.5	24
FMFH	FALSE	17	3	22	25	19.5	25
TC	FALSE	22	20	13	22	21	26
FMEAN	FALSE	26	27	19	2	22.5	27
ShannonEnt	FALSE	29	29	18	6	23.5	28
M2	FALSE	12	25	27	28	26	29

**Table 4.2** Evaluation scores for each feature

Then, feature subsets are generated by adding sorted features incrementally one by one sequentially. The efficiency of each subset is evaluated with six different classification techniques.

Since our dataset is balanced by the number of samples related to each class (121 fall samples and 117 non-fall samples), accuracy percentages are considered as a suitable measurement unit to evaluate the results and compare algorithms.

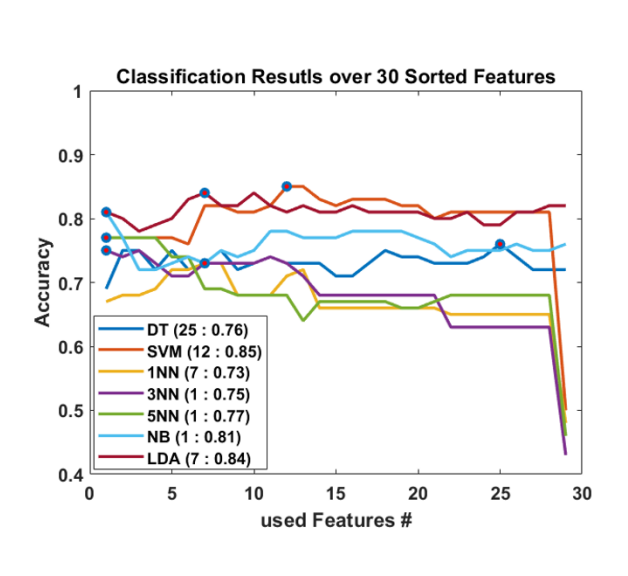
Sorting features according to their importance is an effective technique to determine the best feature subset for each learning method. Figure 4.4 presents average accuracy scores for six different learning models with each feature subset. For this evaluation 5-Fold cross-validation technique has been evaluated over the train set. According to obtained results, selected features various according to the used learning method as it is 7 feature for kNN with average accuracy of 73%, one feature for NB with 81% accuracy, 7 feature for LDA with 84%, 12 features for SVM with 85%, and 25 features for DT with 76%.

The obtained classification results clearly show the effect of the correlation between the features. It is evident that after the 15'th feature, the accuracy does not exhibit major changes by adding more features because most of these features are correlated to the previous used features. Also, it is observed that M2 (the variance of the frequency) has very negative effect on classification results of kNN and SVM algorithms; and the reason behind this is clarified by the following points:

- Welch's method is used for computing M2. This method aims to reduce the noise which leads to a reduction in the frequency resolution [110]. This is causing samples from different classes to have very similar (almost same) variances. So, differentiating between fall and non-fall samples using this features is very poor.
- SVM and kNN algorithms are not immune to poor quality features and does not have built-in feature selection techniques. Thus, they are effected by M2 and their accuracy have shown a sharp drop.

In the previous analyses, the features have been sorted by their importance. By this, poor features got lower scores and M2 got the lowest score between them all. This proves the importance of feature evaluating step that helped in detecting and eliminating low quality features in a very effective way.

After selecting the best features to be used for different learning methods. The next step is to select the classification model that best suits our dataset. For this end, generated models are tested to examine if there is an overfitting problem by comparing their performance over validation, train and test sets. Intentionally, all previous evaluations have been done over train and validation sets that are 80% of the dataset,



Sorted	Classification Results						
Features	3-NN	5-NN	NB	1-NN	LDA	SVM	DT
ENTROPY	0.75	0.77	0.81	0.67	0.81	0.77	0.69
POWER	0.74	0.77	0.77	0.68	0.80	0.77	0.75
DURATION	0.75	0.77	0.72	0.68	0.78	0.77	0.75
FB1FB2	0.73	0.77	0.72	0.69	0.79	0.77	0.72
EX	0.71	0.74	0.73	0.72	0.80	0.77	0.75
ZCR	0.71	0.74	0.74	0.72	0.83	0.76	0.72
FB1	0.73	0.69	0.73	0.73	0.84	0.82	0.73
МОВ	0.73	0.69	0.75	0.73	0.82	0.82	0.75
FB2	0.73	0.68	0.74	0.68	0.82	0.81	0.72
MEDIAN	0.73	0.68	0.75	0.68	0.84	0.81	0.73
SKEW	0.74	0.68	0.78	0.68	0.82	0.82	0.74
KURT	0.73	0.68	0.78	0.71	0.81	0.85	0.73
FL	0.71	0.64	0.77	0.72	0.82	0.85	0.73
FM	0.68	0.67	0.77	0.66	0.81	0.83	0.73
FLFM	0.68	0.67	0.77	0.66	0.81	0.82	0.71
CORR	0.68	0.67	0.78	0.66	0.82	0.83	0.71
RMS	0.68	0.67	0.78	0.66	0.81	0.83	0.73
MEAN	0.68	0.67	0.78	0.66	0.81	0.83	0.75
M3	0.68	0.66	0.78	0.66	0.81	0.82	0.74
V	0.68	0.66	0.77	0.66	0.81	0.82	0.74
FLFH	0.68	0.67	0.76	0.66	0.80	0.80	0.73
FH	0.63	0.68	0.74	0.65	0.80	0.81	0.73
FF	0.63	0.68	0.75	0.65	0.81	0.81	0.73
FMED	0.63	0.68	0.75	0.65	0.79	0.81	0.74
FMFH	0.63	0.68	0.75	0.65	0.79	0.81	0.76
TC	0.63	0.68	0.76	0.65	0.81	0.81	0.74
FMEAN	0.63	0.68	0.75	0.65	0.81	0.81	0.72
ShannonEnt	0.63	0.68	0.75	0.65	0.82	0.81	0.72
M2	0.43	0.46	0.76	0.48	0.82	0.50	0.72

Figure 4.4 Classification results with 30 sorted features

while test set has been left to the last step to evaluate the model performance over new/unseen data samples. However, to have more realistic results the selection of the test set is randomly repeated three times and three randomly selected test sets named as; testSet1, testSet2 and testSet3 are evaluated. Classification results are first evaluated according to each test set separately, then the final evaluation is made according to the average scores.

To compare classification models performance, Receiver Operator Characteristic (ROC) and the Area Under the Curve (AUC) are used, as they summarize the trade-off between the true positive rate (TPR) and false positive rate (FPR) for each model using different probability thresholds. TPR is the proportion of fall samples that are correctly classified and is also known as Recall or Sensitivity. Even though some methods does not have hyper parameters to be evaluated, ROC curves still present a good technique to compare different classification models. ROC curves and AUC scores for selected classification model on the testSet3 are shown in figure 4.5.

ROC and AUC results on the test set show that SVM, LDA, and NB have better classification performance than kNN and DT. However, to examine the number of the samples that have been missclassified by each model, the confusion matrix on each test set is presented in figure 4.6.

By observing confusion matrices for each model on each test set, it is observed that LDA has better in detecting fall events, since the number of the missed falls is less

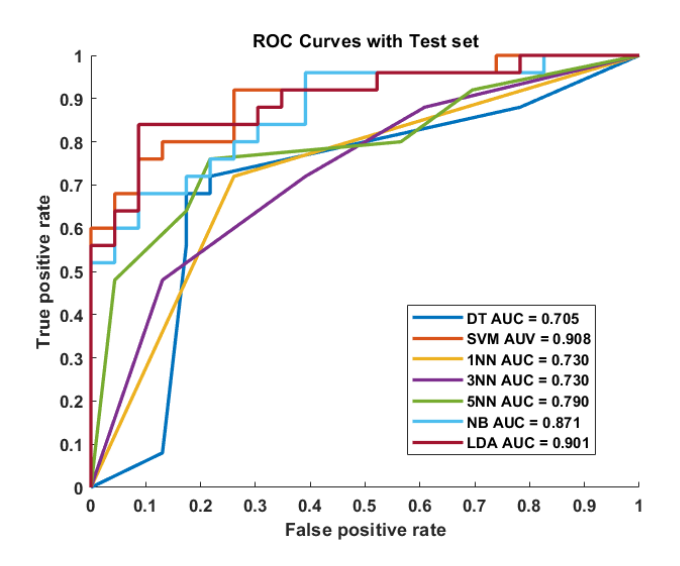


Figure 4.5 ROC curves and AUC scores for different classifiers on testSet3

compared to the other models.

Moreover, important evaluation metrics are extracted from confusion matrices and used for comparing the models, computed evaluation matrices are:

• *Precision:* shows how accurate the model is out of predicted positive samples (how many falls are actual falls).

$$Precision = \frac{TruePositive}{TruePositive + FalsePositive}$$
(4.3)

• *Recall:* calculates how many of the actual Positives the model detected them as Positive (how many falls are detected from actual falls).

$$Recall = \frac{TruePositive}{TruePositive + FalseNegative}$$
(4.4)

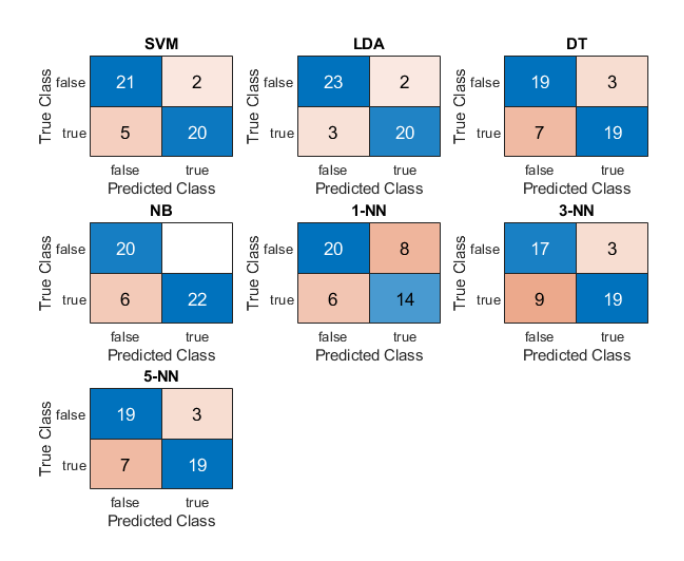
• F1 Score: is also computed as a balance between Precision and Recall.

$$F_1 = 2 * \frac{Precision * Recall}{Precision + Recall}$$
(4.5)

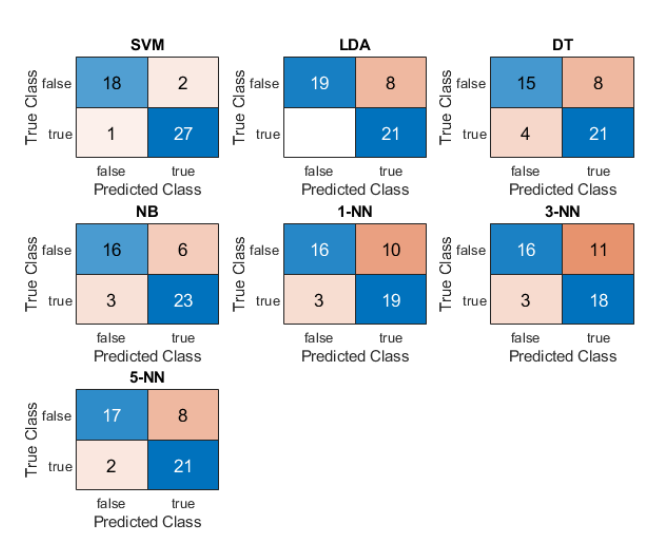
• Accuracy: calculates how many samples are correctly classified.

$$Accuracy = \frac{TruePositive + TrueNegative}{TruePositive + TrueNegative + FalsePositive + FalseNegative}. \tag{4.6}$$

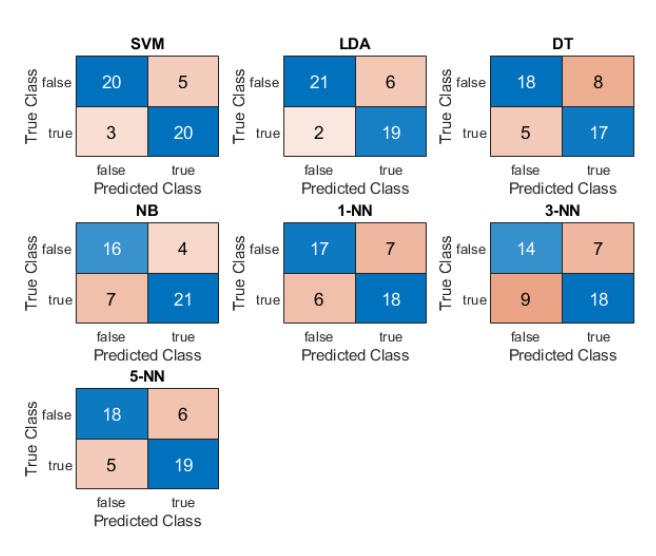
• Specificity: calculates how many of the actual Negatives in are classified as



#### (a) Confusion matrices on testSet1



#### (b) Confusion matrices on testSet2



### (c) Confusion matrices on testSet3

Figure 4.6 Confusion matrices for fall detecting using different classifiers

Negatives (how many non-falls are are correctly classified).

$$Specificity = \frac{TrueNegative}{TrueNegative + FalsePositive}$$
(4.7)

Table 4.3, table 4.4, and table 4.5 presents precision, recall, accuracy, specificity, and f1 scores for each classification model over each test set.

**Table 4.3** Evaluating results with different metrics on testSet1

	Precision	Recall	F1 score	Accuracy	Specificity
DT	0.86	0.73	0.79	0.79	0.86
SVM	0.91	0.80	0.85	0.85	0.91
1-NN	0.64	0.70	0.67	0.71	0.71
3-NN	0.86	0.68	0.76	0.75	0.85
5-NN	0.86	0.73	0.79	0.79	0.86
NB	1.00	0.79	0.88	0.88	1.00
LDA	0.91	0.87	0.89	0.90	0.92

**Table 4.4** Evaluating results with different metrics on testSet2

	Precision	Recall	F1 score	Accuracy	Specificity
DT	0.72	0.84	0.78	0.75	0.65
SVM	0.93	0.96	0.95	0.94	0.90
1-NN	0.66	0.86	0.75	0.73	0.62
3-NN	0.62	0.86	0.72	0.71	0.59
5-NN	0.72	0.91	0.81	0.79	0.68
NB	0.79	0.88	0.84	0.81	0.73
LDA	0.72	1.00	0.84	0.83	0.70

**Table 4.5** Evaluating results with different metrics on testSet3

	Precision	Recall	F1 score	Accuracy	Specificity
DT	0.69	0.73	0.72	0.77	0.68
SVM	0.80	0.83	0.83	0.87	0.80
1-NN	0.71	0.73	0.73	0.75	0.72
3-NN	0.67	0.67	0.69	0.67	0.72
5-NN	0.75	0.77	0.78	0.79	0.76
NB	0.80	0.77	0.79	0.75	0.84
LDA	0.78	0.83	0.83	0.90	0.76

By taking the average of the results on the three test sets for each model, an average metric result is computed and used to decide the machine learning model that is the most suitable for this problem and the collected data. Average results are presented in table 4.6.

Evaluation results show that SVM has provided higher precision, F1 score, accuracy and specificity percentages, whereas, LDA has provided higher Recall percentages.

**Table 4.6** The average of evaluating results on the three test sets

	Precision	Recall	F1 score	Accuracy	Specificity
DT	0.76	0.77	0.76	0.77	0.73
SVM	0.88	0.87	0.88	0.89	0.87
1-NN	0.67	0.76	0.72	0.73	0.68
3-NN	0.72	0.73	0.72	0.71	0.72
5-NN	0.78	0.80	0.79	0.79	0.77
NB	0.86	0.81	0.84	0.81	0.86
LDA	0.80	0.90	0.85	0.88	0.79

For fall detection problem, False Negatives are considered to have high cost, thus, among the evaluation metrics, Recall results are important to be more considered. Additionally, LDA model has been trained with 7 features, whereas, SVM has been trained with 12 features. Thus, LDA has been considered as the most suitable machine learning method for this problem.

### 4.3 Conclusion and Recommendations

Monitoring elderly home activities is important for mitigating health care costs and ensuring the safety of the elders while being alone at home. Consequences of falling accidents are considered as one of the most harmful things for elderly people. According to the fact that most of elderly falls occur in low and middle income segments, in this work, low price radar-based system for elderly activity classification and fall detection has been proposed as a solution for this problem. Several advantages made the radar an ideal candidate for this work as it is contactless, safe and privacy compliant for monitoring individuals. Moreover, it has very low cost (less than \$10) which makes the system affordable for the lower income segment.

In literature there are very few demonstrations of single CW Doppler radar systems capable of observing elder activities in order to detect fall events and examine the status of the fallen person after the fall. Moreover, most of the proposed fall detection systems did not consider falls related to bed room scenarios, although 50% of elderly falls at home are recorded and proven to be in bed room. Thus, proposed system is especially developed to examine bed room's fall situations and it is further expanded to monitor the vital signs of the fallen person in order to analyse its status after the fall. For this end, different algorithms for vital signs extraction, activity monitoring and fall detection were presented. Sliding RMS method is used to detect the major physical activities. Then, linear SVM technique is utilized to classify the activities from a collected dataset of 238 samples in two classes: falls and non-falls related activities. On the other hand, for vital signs detection, peak counting methods have

been developed. The system showed promising classification and monitoring accuracy results which are 88%, 95%, and 85% for falls detection, heartbeat rate and resperation rate respectively.

In this work, for activity classification, features from frequency and time domain were extracted independently. So, it is recommended that in future works, classifier performance with time-frequency features using short time Fourier transform (STFT) or wavelet transform to be examined.

In this work, while collecting the data, there was no spatial session to analyze the effect of different noise types. For future studies, the effect of different noise sources in the uncontrolled environment should be considered.

Because it is not an option to gather data related to actual elder falls in the very first step while designing the system, classification model was trained by data collected from actors which may not represent real data well. Thus, to improve the robustness of classification model, uncontrolled data collection is planned to take place in future studies. A single radar unit will be placed in an elder's bed room along with a reference sensor and then collected data will be used to retrain and update the classifier. Moreover, in future works, we plan to investigate the placement of a single sensor in different places at home including bathroom, kitchen, and living room.

This research clearly illustrates that it is possible to detect falls without limitations of the light conditions, covers, or privacy concerns. Although the system relays on the assumption that the need of fall detection is especially for the cases when the elder person is alone at home, in future works, the occupancy of more than one person in the room could be monitored by applying data fusion using CW and UWB radar. More importantly, future works should involve separating the signals related to human's movements from the ones related to pets' movements. To identify the number of individuals in a specific area of the room, time domain decomposition techniques, such as empirical mode decomposition (EMD), could be used.

Finally, based on our extensive experiments and analysis of different fall types, it can be concluded that radar position and the distance between the radar and the person are important factors to be considered while designing and monitoring the system. Our results indicate that placing the radar on the ceiling of the experiment area with distance within 2,5 meters ensures more valid and accurate detection and monitoring results. Examining two different bed heights showed that falls from the lower bed are more likely to be missed, yet, the height of the bed is only 45 cm and it has less risk of causing damage in the fall case, while falls from bed with 60 cm height are clearer and more detectable by the system.

Based on these conclusions, practitioners should carefully consider the field of view of the used radar and manage the radar place, direction, distance, and number to cover the whole area in the place.

# A EXTRACTED FEATURES

Table A.1 presents the extracted features with their description and used abbreviation within the work.

**Table A.1** Details of the extracted features

Feature Name	Description	Abbreviation
Time	Domain Features (13 features)	
Correlation of whole signal	correlation between time series window and a delayed version of it.	CORR
Root Mean Square	average power of radar signal	RMS
Zero Crossing Rate	times the signal crosses zero.	ZCR
Turns Count	number of zero-crossing of the first derivative	TC
3 Central Moments (Second, Third, Forth)	Variance, Skewness, Kurtosis	v, skew, kurt
Mobility	square root of first derivative's variance, divided by variance of the signal	МОВ
Form Factor	the ratio of the RMS value to the average value	FF
ENTROPY	uncertainty amount or randomness in the pattern	ENTROPY
Mean	the mean of the window	Mean
Median	the median of the window	Median
POWER	sum of absolute squares of samples divided by the signal length	POWER
Frequer	ncy Domain Features (45 features)	
Total Power	the distribution of power into frequency components composing that signal	EX
4 Spectral Moments	Mean Frequency, Median Frequency	FMEAN, FMED
(First, Second, Third, Forth)	FVariance, FSkewness	M2, M3
Energy of Welch Periodogram normalized by the energy of entire spectrum	Band1 [0.167,0.33] Hz Band2 [0.33, 0.67] Hz	FB1 FB2
Ratio of Energy	FB1/FB2	FB1FB2
SHANNON Entropy	spectral power distribution	SHANNONEnt

Additionally, spectral power for different frequency bands are evaluated. Features related to spectral power are represented in table A.2.

 Table A.2 Features extracted from spectral power

Feature Name	Description	Abbreviation				
Spectral Power features group1						
Spectral Power Fractions (SPF) (8 Bands)	Band1[0.2,0.667 Hz], Band2[0.667,3 Hz], Band3[3,5 Hz], Band4[5,8 Hz], Band5[8,11 Hz], Band6[11,18Hz], Band7[18,25 Hz], Band8[>25 Hz]	F1, F2 F3, F4 F5, F6 F7, F8				
Spectral Power Ratios (SPR) (28 Ratios)	F1/F2, F1/F3, F1/F4, F1/F5, F1/F6, F1/F7,F1/F8, F2/F3, F2/F4, F2/F5, F2/F6, F2/F7,F2/F8, F3/F4, F3/F5, F3/F6, F3/F7, F3/F8,F4/F5, F4/F7, F4/F8, F5/F6, F5/F7,F5/F8, F6/F7, F6/F8, F7/F8	F1F2, F1F3, F1F4, F1F5, F1F6, F1F7, F1F8, F2F3, F2F4, F2F5, F2F6, F2F7, F2F8, F3F4, F3F5, F3F6, F3F7, F3F8, F4,F5, F4F6, F4F7, F4F8, F5F6, F5F7, F5F8, F6F7, F6F8, F7F8				
Spectral Power features group2						
Spectral Power Fractions	Band1[0.5,5 Hz], Band2[5,15 Hz]	FL, FM,				
(SPF) (3 Bands)	Band3[>15 Hz]	FH				
Spectral Power Ratios	FL/FM,	FLFM,				
(SPR) (3 Ratios)	FL/FH, FM/FH	FLFM, FMFH				

- [1] S. Sadigh, A. Reimers, R. Andersson, and L. Laflamme, "Falls and fall-related injuries among the elderly: A survey of residential-care facilities in a swedish municipality," *Journal of community health*, vol. 29, no. 2, pp. 129–140, 2004.
- [2] M. G. Amin, Y. D. Zhang, F. Ahmad, and K. D. Ho, "Radar signal processing for elderly fall detection: The future for in-home monitoring," *IEEE Signal Processing Magazine*, vol. 33, no. 2, pp. 71–80, 2016.
- [3] S. L. Murphy, J. Xu, K. D. Kochanek, S. Curtin, and E. Elizabeth Arias, "National vital statistics reports," *National Center for Health Statistics*, 2000.
- [4] E. E. Stone, M. Skubic, M. Rantz, and M. Popescu, Activity analysis, fall detection and risk assessment systems and methods, US Patent 9,597,016, Mar. 2017.
- [5] J. Stevens, D. Rose, K. Cameron, et al., "Falls free: Promoting a national falls prevention action plan," Research Review Papers. Washington DC: National Council on Aging Falls Free Initiative, 2005.
- [6] M. C. Chuah and F. Fu, "Ecg anomaly detection via time series analysis," in *International Symposium on Parallel and Distributed Processing and Applications*, Springer, 2007, pp. 123–135.
- [7] U. Lindemann, A. Hock, M. Stuber, W. Keck, and C. Becker, "Evaluation of a fall detector based on accelerometers: A pilot study," *Medical and Biological engineering and computing*, vol. 43, no. 5, pp. 548–551, 2005.
- [8] R. Igual, C. Medrano, and I. Plaza, "Challenges, issues and trends in fall detection systems," *Biomedical engineering online*, vol. 12, no. 1, p. 66, 2013.
- [9] P. Setlur, M. G. Amin, F. Ahmad, and P. D. Zemany, "Experiments on through-the-wall motion detection and ranging," in *Sensors, and Command, Control, Communications, and Intelligence (C3I) Technologies for Homeland Security and Homeland Defense VI*, International Society for Optics and Photonics, vol. 6538, 2007, p. 653809.
- [10] Q. Wu, Y. D. Zhang, W. Tao, and M. G. Amin, "Radar-based fall detection based on doppler time–frequency signatures for assisted living," *IET Radar, Sonar & Navigation*, vol. 9, no. 2, pp. 164–172, 2015.
- [11] E. S. F. Coutinho, K. V. Bloch, and L. C. Rodrigues, "Characteristics and circumstances of falls leading to severe fractures in elderly people in rio de janeiro, brazil," *Cadernos de saude publica*, vol. 25, pp. 455–459, 2009.
- [12] X. Yu, "Approaches and principles of fall detection for elderly and patient," in *HealthCom 2008-10th International Conference on e-health Networking, Applications and Services*, IEEE, 2008, pp. 42–47.

- [13] M. Mubashir, L. Shao, and L. Seed, "A survey on fall detection: Principles and approaches," *Neurocomputing*, vol. 100, pp. 144–152, 2013.
- [14] C. J. Lord and D. P. Colvin, "Falls in the elderly: Detection and assessment," in *Proceedings of the Annual International Conference of the IEEE Engineering in Medicine and Biology Society Volume 13: 1991*, IEEE, 1991, pp. 1938–1939.
- [15] G. Williams, K. Doughty, K. Cameron, and D. Bradley, "A smart fall and activity monitor for telecare applications," in *Proceedings of the 20th Annual International Conference of the IEEE Engineering in Medicine and Biology Society.* Vol. 20 Biomedical Engineering Towards the Year 2000 and Beyond (Cat. No. 98CH36286), IEEE, vol. 3, 1998, pp. 1151–1154.
- [16] T. Zhang, J. Wang, P. Liu, and J. Hou, "Fall detection by embedding an accelerometer in cellphone and using kfd algorithm," *International Journal of Computer Science and Network Security*, vol. 6, no. 10, pp. 277–284, 2006.
- [17] A. Sucerquia, J. López, and J. Vargas-Bonilla, "Real-life/real-time elderly fall detection with a triaxial accelerometer," *Sensors*, vol. 18, no. 4, p. 1101, 2018.
- [18] M. Prado, J. Reina-Tosina, and L. Roa, "Distributed intelligent architecture for falling detection and physical activity analysis in the elderly," in *Proceedings of the Second Joint 24th Annual Conference and the Annual Fall Meeting of the Biomedical Engineering Society* [Engineering in Medicine and Biology, IEEE, vol. 3, 2002, pp. 1910–1911.
- [19] M. Alwan, P. J. Rajendran, S. Kell, D. Mack, S. Dalal, M. Wolfe, and R. Felder, "A smart and passive floor-vibration based fall detector for elderly," in *Information and Communication Technologies*, vol. 1, 2006, pp. 1003–1007.
- [20] G. Feng, J. Mai, Z. Ban, X. Guo, and G. Wang, "Floor pressure imaging for fall detection with fiber-optic sensors," *IEEE Pervasive Computing*, vol. 15, no. 2, pp. 40–47, 2016.
- [21] A. Sixsmith and N. Johnson, "A smart sensor to detect the falls of the elderly," *IEEE Pervasive computing*, vol. 3, no. 2, pp. 42–47, 2004.
- [22] A. Sixsmith, N. Johnson, and R. Whatmore, "Pyroelectric ir sensor arrays for fall detection in the older population," in *Journal de Physique IV (Proceedings)*, EDP sciences, vol. 128, 2005, pp. 153–160.
- [23] G. Wu, "Distinguishing fall activities from normal activities by velocity characteristics," *Journal of biomechanics*, vol. 33, no. 11, pp. 1497–1500, 2000.
- [24] C. Rougier, J. Meunier, *et al.*, "Fall detection using 3d head trajectory extracted from a single camera video sequence," in *First International Workshop on Video Processing for Security (VP4S-06), June*, 2006, pp. 7–9.
- [25] H. Nait-Charif and S. J. McKenna, "Activity summarisation and fall detection in a supportive home environment," in *Proceedings of the 17th International Conference on Pattern Recognition, 2004. ICPR 2004.*, IEEE, vol. 4, 2004, pp. 323–326.
- [26] M. Ko, S. Kim, M. Kim, and K. Kim, "A novel approach for outdoor fall detection using multidimensional features from a single camera," *Applied Sciences*, vol. 8, no. 6, p. 984, 2018.

- [27] E. E. Stone and M. Skubic, "Fall detection in homes of older adults using the microsoft kinect," *IEEE journal of biomedical and health informatics*, vol. 19, no. 1, pp. 290–301, 2014.
- [28] G. Mastorakis and D. Makris, "Fall detection system using kinect's infrared sensor," *Journal of Real-Time Image Processing*, vol. 9, no. 4, pp. 635–646, 2014.
- [29] B. Kwolek and M. Kepski, "Human fall detection on embedded platform using depth maps and wireless accelerometer," *Computer methods and programs in biomedicine*, vol. 117, no. 3, pp. 489–501, 2014.
- [30] J. Wang, Z. Zhang, B. Li, S. Lee, and R. S. Sherratt, "An enhanced fall detection system for elderly person monitoring using consumer home networks," *IEEE transactions on consumer electronics*, vol. 60, no. 1, pp. 23–29, 2014.
- [31] S. Gasparrini, E. Cippitelli, S. Spinsante, and E. Gambi, "A depth-based fall detection system using a kinect (R) sensor," *Sensors*, vol. 14, no. 2, pp. 2756–2775, 2014.
- [32] X. Ma, H. Wang, B. Xue, M. Zhou, B. Ji, and Y. Li, "Depth-based human fall detection via shape features and improved extreme learning machine," *IEEE journal of biomedical and health informatics*, vol. 18, no. 6, pp. 1915–1922, 2014.
- [33] Z.-P. Bian, J. Hou, L.-P. Chau, and N. Magnenat-Thalmann, "Fall detection based on body part tracking using a depth camera," *IEEE journal of biomedical and health informatics*, vol. 19, no. 2, pp. 430–439, 2014.
- [34] M. G. Amin, Y. D. Zhang, F. Ahmad, and K. D. Ho, "Radar signal processing for elderly fall detection: The future for in-home monitoring," *IEEE Signal Processing Magazine*, vol. 33, no. 2, pp. 71–80, 2016.
- [35] B. Y. Su, K. Ho, M. J. Rantz, and M. Skubic, "Doppler radar fall activity detection using the wavelet transform," *IEEE Transactions on Biomedical Engineering*, vol. 62, no. 3, pp. 865–875, 2014.
- [36] L.-J. Kau and C.-S. Chen, "A smart phone-based pocket fall accident detection, positioning, and rescue system," *IEEE journal of biomedical and health informatics*, vol. 19, no. 1, pp. 44–56, 2014.
- [37] B. Kwolek and M. Kepski, "Improving fall detection by the use of depth sensor and accelerometer," *Neurocomputing*, vol. 168, pp. 637–645, 2015.
- [38] B. Jokanovic, M. Amin, and F. Ahmad, "Radar fall motion detection using deep learning," in *2016 IEEE radar conference (RadarConf)*, IEEE, 2016, pp. 1–6.
- [39] M. Kepski and B. Kwolek, "Fall detection using ceiling-mounted 3d depth camera," in *2014 International conference on computer vision theory and applications (VISAPP)*, IEEE, vol. 2, 2014, pp. 640–647.
- [40] J. K. Lee, S. N. Robinovitch, and E. J. Park, "Inertial sensing-based pre-impact detection of falls involving near-fall scenarios," *IEEE transactions on neural systems and rehabilitation engineering*, vol. 23, no. 2, pp. 258–266, 2014.

- [41] J. C. Castillo, D. Carneiro, J. Serrano-Cuerda, P. Novais, A. Fernández-Caballero, and J. Neves, "A multi-modal approach for activity classification and fall detection," *International Journal of Systems Science*, vol. 45, no. 4, pp. 810–824, 2014.
- [42] Y. Li, K. Ho, and M. Popescu, "Efficient source separation algorithms for acoustic fall detection using a microsoft kinect," *IEEE Transactions on Biomedical Engineering*, vol. 61, no. 3, pp. 745–755, 2013.
- [43] J. Liu and T. E. Lockhart, "Development and evaluation of a prior-to-impact fall event detection algorithm," *IEEE Transactions on Biomedical Engineering*, vol. 61, no. 7, pp. 2135–2140, 2014.
- [44] B. Aguiar, T. Rocha, J. Silva, and I. Sousa, "Accelerometer-based fall detection for smartphones," in *2014 IEEE International Symposium on Medical Measurements and Applications (MeMeA)*, IEEE, 2014, pp. 1–6.
- [45] J.-L. Chua, Y. C. Chang, and W. K. Lim, "A simple vision-based fall detection technique for indoor video surveillance," *Signal, Image and Video Processing*, vol. 9, no. 3, pp. 623–633, 2015.
- [46] T. Xu, Y. Zhou, and J. Zhu, "New advances and challenges of fall detection systems: A survey," *Applied Sciences*, vol. 8, no. 3, p. 418, 2018.
- [47] F. Bagalà, C. Becker, A. Cappello, L. Chiari, K. Aminian, J. M. Hausdorff, W. Zijlstra, and J. Klenk, "Evaluation of accelerometer-based fall detection algorithms on real-world falls," *PloS one*, vol. 7, no. 5, e37062, 2012.
- [48] H. Jiang, C. Cai, X. Ma, Y. Yang, and J. Liu, "Smart home based on wifi sensing: A survey," *IEEE Access*, vol. 6, pp. 13317–13325, 2018.
- [49] P. Setlur, M. G. Amin, F. Ahmad, and P. D. Zemany, "Experiments on through-the-wall motion detection and ranging," in *Sensors, and Command, Control, Communications, and Intelligence (C3I) Technologies for Homeland Security and Homeland Defense VI*, International Society for Optics and Photonics, vol. 6538, 2007, p. 653809.
- [50] L. Liu, M. Popescu, M. Skubic, M. Rantz, T. Yardibi, and P. Cuddihy, "Automatic fall detection based on doppler radar motion signature," in *2011 5th International Conference on Pervasive Computing Technologies for Healthcare (PervasiveHealth) and Workshops*, IEEE, 2011, pp. 222–225.
- [51] S. Tomi and T. Ohtsuki, "Falling detection using multiple doppler sensors," in 2012 IEEE 14th International Conference on e-Health Networking, Applications and Services (Healthcom), IEEE, 2012, pp. 196–201.
- [52] S. Tomii and T. Ohtsuki, "Falling detection using multiple doppler sensors," in 2012 IEEE 14th International Conference on e-Health Networking, Applications and Services (Healthcom), IEEE, 2012, pp. 196–201.
- [53] F. Wang, M. Skubic, M. Rantz, and P. E. Cuddihy, "Quantitative gait measurement with pulse-doppler radar for passive in-home gait assessment," *IEEE Transactions on Biomedical Engineering*, vol. 61, no. 9, pp. 2434–2443, 2014.

- [54] A. Gadde, M. G. Amin, Y. D. Zhang, and F. Ahmad, "Fall detection and classifications based on time-scale radar signal characteristics," in *Radar Sensor Technology XVIII*, International Society for Optics and Photonics, vol. 9077, 2014, p. 907712.
- [55] Q. Wu, Y. D. Zhang, W. Tao, and M. G. Amin, "Radar-based fall detection based on doppler time–frequency signatures for assisted living," *IET Radar, Sonar & Navigation*, vol. 9, no. 2, pp. 164–172, 2015.
- [56] B. Y. Su, K. Ho, M. J. Rantz, and M. Skubic, "Doppler radar fall activity detection using the wavelet transform," *IEEE Transactions on Biomedical Engineering*, vol. 62, no. 3, pp. 865–875, 2014.
- [57] L. Liu, M. Popescu, M. Skubic, M. Rantz, T. Yardibi, and P. Cuddihy, "Automatic fall detection based on doppler radar motion signature," in 2011 5th International Conference on Pervasive Computing Technologies for Healthcare (PervasiveHealth) and Workshops, IEEE, 2011, pp. 222–225.
- [58] L. Liu, M. Popescu, M. Rantz, and M. Skubic, "Fall detection using doppler radar and classifier fusion," in *Proceedings of 2012 IEEE-EMBS International Conference on Biomedical and Health Informatics*, IEEE, 2012, pp. 180–183.
- [59] L. Liu, M. Popescu, M. Skubic, M. Rantz, and P. Cuddihy, "An automatic in-home fall detection system using doppler radar signatures," *Journal of Ambient Intelligence and Smart Environments*, vol. 8, no. 4, pp. 453–466, 2016.
- [60] J. Sachs and R. Herrmann, "M-sequence-based ultra-wideband sensor network for vitality monitoring of elders at home," *IET Radar, Sonar & Navigation*, vol. 9, no. 2, pp. 125–137, 2015.
- [61] Z. Cammenga, G. Smith, and C. Baker, "Combined high range resolution and micro-doppler analysis of human gait," in *2015 IEEE Radar Conference (Radar-Con)*, IEEE, 2015, pp. 1038–1043.
- [62] P. J. Soh, M. Mercuri, G. Pandey, G. A. Vandenbosch, and D. M.-P. Schreurs, "Dual-band planar bowtie monopole for a fall-detection radar and telemetry system," *IEEE Antennas and Wireless Propagation Letters*, vol. 11, pp. 1698–1701, 2012.
- [63] M. Mercuri, P. J. Soh, G. Pandey, P. Karsmakers, G. A. Vandenbosch, P. Leroux, and D. Schreurs, "Analysis of an indoor biomedical radar-based system for health monitoring," *IEEE Transactions on Microwave Theory and Techniques*, vol. 61, no. 5, pp. 2061–2068, 2013.
- [64] P. Karsmakers, T. Croonenborghs, M. Mercuri, D. Schreurs, and P. Leroux, "Automatic in-door fall detection based on microwave radar measurements," in *2012 9th European Radar Conference*, IEEE, 2012, pp. 202–205.
- [65] M. Mercuri, P. J. Soh, L. Boccia, D. Schreurs, G. A. Vandenbosch, P. Leroux, and G. Amendola, "Optimized sfcw radar sensor aiming at fall detection in a real room environment," in 2013 IEEE Topical Conference on Biomedical Wireless Technologies, Networks, and Sensing Systems, IEEE, 2013, pp. 4–6.
- [66] J. Hong, S. Tomii, and T. Ohtsuki, "Cooperative fall detection using doppler radar and array sensor," in *2013 IEEE 24th Annual International Symposium on Personal, Indoor, and Mobile Radio Communications (PIMRC)*, IEEE, 2013, pp. 3492–3496.

- [67] M. Wu, X. Dai, Y. D. Zhang, B. Davidson, M. G. Amin, and J. Zhang, "Fall detection based on sequential modeling of radar signal time-frequency features," in *2013 IEEE International Conference on Healthcare Informatics*, IEEE, 2013, pp. 169–174.
- [68] A. Gadde, M. G. Amin, Y. D. Zhang, and F. Ahmad, "Fall detection and classifications based on time-scale radar signal characteristics," in *Radar Sensor Technology XVIII*, International Society for Optics and Photonics, vol. 9077, 2014, p. 907712.
- [69] L. R. Rivera, E. Ulmer, Y. D. Zhang, W. Tao, and M. G. Amin, "Radar-based fall detection exploiting time-frequency features," in *2014 IEEE China Summit & International Conference on Signal and Information Processing (ChinaSIP)*, IEEE, 2014, pp. 713–717.
- [70] M. G. Amin, Y. D. Zhang, and B. Boashash, "High-resolution time-frequency distributions for fall detection," in *Radar Sensor Technology XIX; and Active and Passive Signatures VI*, International Society for Optics and Photonics, vol. 9461, 2015, 94611B.
- [71] Q. Wu, Y. D. Zhang, W. Tao, and M. G. Amin, "Radar-based fall detection based on doppler time–frequency signatures for assisted living," *IET Radar, Sonar & Navigation*, vol. 9, no. 2, pp. 164–172, 2015.
- [72] B. Y. Su, K. Ho, M. J. Rantz, and M. Skubic, "Doppler radar fall activity detection using the wavelet transform," *IEEE Transactions on Biomedical Engineering*, vol. 62, no. 3, pp. 865–875, 2014.
- [73] Z. Peng, J.-M. Muñoz-Ferreras, R. Gómez-Garcia, and C. Li, "Fmcw radar fall detection based on isar processing utilizing the properties of rcs, range, and doppler," in 2016 IEEE Mtt-S International Microwave Symposium (IMS), IEEE, 2016, pp. 1–3.
- [74] H. Wang, L. Ren, E. Mao, and A. E. Fathy, "Phase based motion characteristics measurement for fall detection by using stepped-frequency continuous wave radar," in 2016 IEEE Topical Conference on Biomedical Wireless Technologies, Networks, and Sensing Systems (BioWireleSS), IEEE, 2016, pp. 43–45.
- [75] B. Jokanovic, M. Amin, and F. Ahmad, "Radar fall motion detection using deep learning," in *2016 IEEE radar conference (RadarConf)*, IEEE, 2016, pp. 1–6.
- [76] B. Jokanovic, M. Amin, F. Ahmad, and B. Boashash, "Radar fall detection using principal component analysis," in *Radar Sensor Technology XX*, International Society for Optics and Photonics, vol. 9829, 2016, p. 982919.
- [77] G. Diraco, A. Leone, and P. Siciliano, "Radar sensing technology for fall detection under near real-life conditions," 2016.
- [78] A. Diraco and P. Siciliano, "A fall detector based on ultra-wideband radar sensing," in *Convegno Nazionale Sensori*, Springer, 2016, pp. 373–382.
- [79] B. Erol, M. G. Amin, and B. Boashash, "Range-doppler radar sensor fusion for fall detection," in *2017 IEEE Radar Conference (RadarConf)*, IEEE, 2017, pp. 0819–0824.
- [80] H. Sadreazami, M. Bolic, and S. Rajan, "On the use of ultra wideband radar and stacked lstm-rnn for at home fall detection," in *2018 IEEE Life Sciences Conference (LSC)*, IEEE, 2018, pp. 255–258.

- [81] B. Erol and M. G. Amin, "Radar data cube analysis for fall detection," in 2018 IEEE International Conference on Acoustics, Speech and Signal Processing (ICASSP), IEEE, 2018, pp. 2446–2450.
- [82] B. Erol, M. Amin, F. Ahmad, and B. Boashash, "Radar fall detectors: A comparison," in *Radar Sensor Technology XX*, International Society for Optics and Photonics, vol. 9829, 2016, p. 982918.
- [83] M. I. Skolnik, "Radar handbook," 1970.
- [84] A. Droitcour, V. Lubecke, J. Lin, and O. Boric-Lubecke, "A microwave radio for doppler radar sensing of vital signs," in *2001 IEEE MTT-S International Microwave Sympsoium Digest (Cat. No. 01CH37157)*, IEEE, vol. 1, 2001, pp. 175–178.
- [85] C. Gu, "Short-range noncontact sensors for healthcare and other emerging applications: A review," *Sensors*, vol. 16, no. 8, p. 1169, 2016.
- [86] C. J. Persico, *I/q quadraphase modulator circuit*, US Patent 5,574,755, Nov. 1996.
- [87] S. N. Robinovitch, F. Feldman, Y. Yang, R. Schonnop, P. M. Leung, T. Sarraf, J. Sims-Gould, and M. Loughin, "Video capture of the circumstances of falls in elderly people residing in long-term care: An observational study," *The Lancet*, vol. 381, no. 9860, pp. 47–54, 2013.
- [88] V. C. Chen, The micro-Doppler effect in radar. Artech House, 2019.
- [89] J. Wang, X. Wang, L. Chen, J. Huangfu, C. Li, and L. Ran, "Noncontact distance and amplitude-independent vibration measurement based on an extended dacm algorithm," *IEEE Transactions on Instrumentation and Measurement*, vol. 63, no. 1, pp. 145–153, 2013.
- [90] B.-K. Park, O. Boric-Lubecke, and V. M. Lubecke, "Arctangent demodulation with dc offset compensation in quadrature doppler radar receiver systems," *IEEE transactions on Microwave theory and techniques*, vol. 55, no. 5, pp. 1073–1079, 2007.
- [91] W. Xu, C. Gu, C. Li, and M. Sarrafzadeh, "Robust doppler radar demodulation via compressed sensing," *Electronics Letters*, vol. 48, no. 22, pp. 1428–1430, 2012.
- [92] M. Rahman and C. L. Sobchak, *Dc offset correction for direct conversion receivers*, US Patent 7,603,094, Oct. 2009.
- [93] C. J. Caspersen, K. E. Powell, and G. M. Christenson, "Physical activity, exercise, and physical fitness: Definitions and distinctions for health-related research.," *Public health reports*, vol. 100, no. 2, p. 126, 1985.
- [94] Y. Kim and S. S. Sekhon, "Detection of moving target and localization of clutter using doppler radar on mobile platform," *IEEE Geoscience and Remote Sensing Letters*, vol. 12, no. 5, pp. 1156–1160, 2015.
- [95] R. M. Rangayyan and N. P. Reddy, "Biomedical signal analysis: A case-study approach," *Annals of Biomedical Engineering*, vol. 30, no. 7, pp. 983–983, 2002.

- [96] A. Fuglsang-Frederiksen and A. Månsson, "Analysis of electrical activity of normal muscle in man at different degrees of voluntary effort.," *Journal of Neurology, Neurosurgery & Psychiatry*, vol. 38, no. 7, pp. 683–694, 1975.
- [97] A. V. Totsky, A. A. Zelensky, and V. F. Kravchenko, *Bispectral methods of signal processing: applications in radar, telecommunications and digital image restoration*. Walter de Gruyter GmbH & Co KG, 2014.
- [98] B. Hjorth, "Eeg analysis based on time domain properties," *Electroencephalog-raphy and clinical neurophysiology*, vol. 29, no. 3, pp. 306–310, 1970.
- [99] R. Merletti, A. Gulisashvili, and L. L. Conte, "Estimation of shape characteristics of surface muscle signal spectra from time domain data," *IEEE transactions on biomedical engineering*, vol. 42, no. 8, pp. 769–776, 1995.
- [100] G. R. Johnson, R. J. Adolph, and D. J. Campbell, "Estimation of the severity of aortic valve stenosis by frequency analysis of the murmur," *Journal of the American College of Cardiology*, vol. 1, no. 5, pp. 1315–1323, 1983.
- [101] L. v. d. Maaten and G. Hinton, "Visualizing data using t-sne," *Journal of machine learning research*, vol. 9, no. Nov, pp. 2579–2605, 2008.
- [102] H. Liu and H. Motoda, Feature extraction, construction and selection: A data mining perspective. Springer Science & Business Media, 1998, vol. 453.
- [103] J. Li, K. Cheng, S. Wang, F. Morstatter, R. P. Trevino, J. Tang, and H. Liu, "Feature selection: A data perspective," *ACM Computing Surveys (CSUR)*, vol. 50, no. 6, p. 94, 2018.
- [104] C. Lee and E. Choi, "Bayes error evaluation of the gaussian ml classifier," *IEEE Transactions on Geoscience and Remote Sensing*, vol. 38, no. 3, pp. 1471–1475, 2000.
- [105] J. D. Rodriguez, A. Perez, and J. A. Lozano, "Sensitivity analysis of k-fold cross validation in prediction error estimation," *IEEE transactions on pattern analysis and machine intelligence*, vol. 32, no. 3, pp. 569–575, 2009.
- [106] C. C. Aggarwal, Data classification: algorithms and applications. CRC press, 2014.
- [107] F. Lotte, M. Congedo, A. Lécuyer, F. Lamarche, and B. Arnaldi, "A review of classification algorithms for eeg-based brain–computer interfaces," *Journal of neural engineering*, vol. 4, no. 2, R1, 2007.
- [108] D. McKechan, C. Robinson, and B. S. Sathyaprakash, "A tapering window for time-domain templates and simulated signals in the detection of gravitational waves from coalescing compact binaries," *Classical and Quantum Gravity*, vol. 27, no. 8, p. 084 020, 2010.
- [109] H. Kemis, N. Bruce, W. Ping, T. Antonio, L. B. Gook, and H. J. Lee, "Healthcare monitoring application in ubiquitous sensor network: Design and implementation based on pulse sensor with arduino," in 2012 6th International Conference on New Trends in Information Science, Service Science and Data Mining (ISSDM2012), IEEE, 2012, pp. 34–38.
- [110] K. J. Seats, J. F. Lawrence, and G. A. Prieto, "Improved ambient noise correlation functions using welch s method," *Geophysical Journal International*, vol. 188, no. 2, pp. 513–523, 2012.

# **PUBLICATIONS from the THESIS**

Contact Information: khadija.hanifi@hotmail.com

# **Papers**

1. K. Hanifi and M. E. Karsligil, "Contactless vital signs monitoring using Doppler radar sensor," Journal of Advances in Technology and Engineering Research, vol. 5, no. 2, pp. 2414–4592, 2019.